Fraunhofer
ITWM

J. Linn, H. Lang, A. Tuganov

Derivation of a viscoelastic constitutive model of Kelvin-Voigt type for Cosserat rods

Vorwort

Das Tätigkeitsfeld des Fraunhofer-Instituts für Techno- und Wirtschaftsmathematik ITWM umfasst anwendungsnahe Grundlagenforschung, angewandte Forschung sowie Beratung und kundenspezifische Lösungen auf allen Gebieten, die für Techno- und Wirtschaftsmathematik bedeutsam sind.

In der Reihe »Berichte des Fraunhofer ITWM« soll die Arbeit des Instituts kontinuierlich einer interessierten Öffentlichkeit in Industrie, Wirtschaft und Wissenschaft vorgestellt werden. Durch die enge Verzahnung mit dem Fachbereich Mathematik der Universität Kaiserslautern sowie durch zahlreiche Kooperationen mit internationalen Institutionen und Hochschulen in den Bereichen Ausbildung und Forschung ist ein großes Potenzial für Forschungsberichte vorhanden. In die Berichtreihe werden sowohl hervorragende Diplom- und Projektarbeiten und Dissertationen als auch Forschungsberichte der Institutsmitarbeiter und Institutsgäste zu aktuellen Fragen der Techno- und Wirtschaftsmathematik aufgenommen.

Darüber hinaus bietet die Reihe ein Forum für die Berichterstattung über die zahlreichen Kooperationsprojekte des Instituts mit Partnern aus Industrie und Wirtschaft.

Berichterstattung heißt hier Dokumentation des Transfers aktueller Ergebnisse aus mathematischer Forschungs- und Entwicklungsarbeit in industrielle Anwendungen und Softwareprodukte – und umgekehrt, denn Probleme der Praxis generieren neue interessante mathematische Fragestellungen.

Prof. Dr. Dieter Prätzel-Wolters
Institutsleiter

Kaiserslautern, im Juni 2001

Derivation of a viscoelastic constitutive model of Kelvin–Voigt type for Cosserat rods

Joachim Linn, Holger Lang, Andrey Tuganov

February 18, 2013

Abstract

We present the derivation[1] of a simple viscous damping model of Kelvin–Voigt type for geometrically exact Cosserat rods from three–dimensional continuum theory. Assuming moderate curvature of the rod in its reference configuration, strains remaining small in its deformed configurations, strain rates that vary slowly compared to internal relaxation processes, and a homogeneous and isotropic material, we obtain explicit formulas for the damping parameters of the model in terms of the well known stiffness parameters of the rod and the retardation time constants defined as the ratios of bulk and shear viscosities to the respective elastic moduli. We briefly discuss the range of validity of the Kelvin–Voigt model and illustrate its behaviour for large bending deformations with a numerical example.

Keywords: geometrically exact rods, viscoelasticity, Kelvin–Voigt model, nonlinear structural dynamics

---

[1]This preprint is a modified version of the journal article (Linn et al., 2013) that is based on the paper (Linn et al., 2012) presented at the IMSD 2012 conference.

1 Introduction

Simulation models for computing the transient response of structural members to dynamic excitations should contain a good approach to account for *dissipative effects* in order to be useful in realistic applications. If the structure considered may be treated within the range of *linear* dynamics with small vibration amplitudes, there is a well established set of standard approaches, e.g. Rayleigh damping, or a more general modal damping ansatz, to add such effects on the level of discretized versions of linear elastic structural models (see e.g. Craig and Kurdila, 2006).

In the case of *geometrically exact* structure models for rods and shells (Antman, 2005), such linear approaches are not applicable. Geometrically exact rods, in particular, have a wide range of applications in *flexible multibody dynamics*. We refer to the brief introduction given in ch. 6 of (Géradin and Cardona, 2001) for a summary of the related work published before 2000, and to ch. 15 of (Bauchau, 2011) for a more recent account on this subject. Here the proper way to model viscous damping requires the inclusion of a *frame–indifferent viscoelastic constitutive model* into the continuum formulation of the structure model that is capable of dealing with *large displacements* and *finite rotations* (see Bauchau, Epple and Heo, 2008).

1.1 Viscous Kelvin–Voigt damping for Cosserat rods

In our recent work (Lang et al., 2011), we suggested the possibly simplest model of this kind to introduce *viscous material damping* in our quaternionic reformulation of Simo's dynamic continuum model for Cosserat rods (Simo, 1985). Following general considerations of Antman (2005) about the functional form of viscoelatic constitutive laws for Cosserat rods, we simply added viscous contributions, which we assumed to be proportional to the *rates* of the *material strain measures* $\mathbf{U}(s,t)$ and $\mathbf{V}(s,t)$ of the rod, to the *material stress resultants* $\mathbf{F}(s,t)$ and *stress couples* $\mathbf{M}(s,t)$, resulting in a constitutive model of *Kelvin–Voigt* type:

$$\mathbf{F} = \hat{\mathbb{C}}_F \cdot (\mathbf{V} - \mathbf{V}_0) + \hat{\mathbb{V}}_F \cdot \partial_t \mathbf{V} \ , \ \ \mathbf{M} = \hat{\mathbb{C}}_M \cdot (\mathbf{U} - \mathbf{U}_0) + \hat{\mathbb{V}}_M \cdot \partial_t \mathbf{U} \ . \quad (1)$$

A detailed presentation of the kinematical quantities and dynamic equilibrium equations of a Cosserat rod is given in section 2, Figs. 1, 2, 3 and 4 provide a compact summary.

In the material constitutive equations (1) the elastic properties of the rod are determined by the *effective stiffness parameters* contained in the symmetric 3×3 matrices $\hat{\mathbb{C}}_F$ and $\hat{\mathbb{C}}_M$. For homogeneous isotropic materials,

both matrices are diagonal and given by:

$$\hat{\mathbb{C}}_F = \operatorname{diag}(GA, GA, EA) \;,\quad \hat{\mathbb{C}}_M = \operatorname{diag}(EI_1, EI_2, GI_3)\;, \qquad (2)$$

with stiffness parameters given by the elastic moduli E and G and geometric parameters (area A, geometric moments I_k) of the cross section. In Lang et al. (2011) we assumed a similar structure for the matrices $\hat{\mathbb{V}}_F$ and $\hat{\mathbb{V}}_M$, which determine the viscous response:

$$\hat{\mathbb{V}}_F = \operatorname{diag}(\gamma_{S1}, \gamma_{S2}, \gamma_E)\;,\quad \hat{\mathbb{V}}_M = \operatorname{diag}(\gamma_{B1}, \gamma_{B2}, \gamma_T)\;. \qquad (3)$$

The set of six *effective viscosity parameters* γ_{xx} introduced in (3) represents the *integrated cross-sectional viscous damping behaviour* associated to the basic deformation modes (bending, twisting, transverse shearing and extension) of the rod, in the same way as the well known set of stiffness parameters given above determines the corresponding elastic response.

1.2   Effective damping parameter formulas

However, in Lang et al. (2011) the damping parameters γ_{xx} remained undetermined w.r.t. their specific dependence on material and geometric properties. Considering the special case of homogeneous and isotropic material properties, they certainly cannot be independent, but rather should be mutually related in a similar way as the stiffness parameters of the rod in terms of two material parameters (E,G) and the geometrical quantities (A,I_k) associated to the cross section.

Assuming moderate curvature of the rod in its reference configuration, strains remaining small in its deformed configurations, strain rates that vary slowly compared to internal relaxation processes within the material, and a homogeneous and isotropic material, we will show that they are given by

$$\frac{\gamma_{S1/2}}{A} = \frac{\gamma_T}{I_3} = \eta\,,\quad \frac{\gamma_E}{A} = \frac{\gamma_{B1/2}}{I_{1/2}} = \zeta(1-2\nu)^2 + \frac{4}{3}\eta(1+\nu)^2, \qquad (4)$$

where ζ and η are the *bulk and shear viscosities* of a viscoelastic *Kelvin–Voigt solid* (Lemaitre and Chaboche, 1990) with elastic moduli $E = 2G(1+\nu)$ and G related via *Poisson's ratio* ν.

While the viscous damping of the deformation modes of pure shear type is solely affected by shear viscosity η, extensional and bending deformations are both associated to normal stresses in the direction orthogonal to the cross section, which are damped by a specific combination of both bulk and

shear viscosity that depends on the compressibilty of the material and may be interpreted as *extensional viscosity* parameter

$$\eta_E := \zeta(1-2\nu)^2 + \frac{4}{3}\eta(1+\nu)^2 \ . \tag{5}$$

Introducing the *retardation time* constants $\tau_S = \eta/G$ and $\tau_B = \zeta/K$, which relate the viscosities η and ζ to the shear and bulk moduli G and $3K = E/(1-2\nu)$, as well as the time constant $\tau_E := \eta_E/E = \frac{1}{3}[(1-2\nu)\tau_B + 2(1+\nu)\tau_S]$ relating extensional viscosity to Young's modulus, the formulas (4) may be rewritten equivalently as

$$\frac{\gamma_{S1/2}}{GA} = \frac{\gamma_T}{GI_3} = \tau_S \ , \quad \frac{\gamma_E}{EA} = \frac{\gamma_{B1/2}}{EI_{1/2}} = \tau_E \tag{6}$$

in terms of the stiffness parameters of the rod and the retardation time constants. Interesting special cases of (6) are the simplified expressions $\eta_E = \zeta + \frac{4}{3}\eta$, $\tau_E = \frac{1}{3}(\tau_B + 2\tau_S)$ for completely compressible materials ($\nu = 0$), and $\eta_E = 3\eta$, $\tau_E = \tau_S$ for incompressible materials ($\nu = \frac{1}{2}$).

The relation $\eta_E/\eta = 3$ between shear and extensional viscosity is well known as *Trouton's ratio* for incompressible Newtonian fluids (Trouton, 1906) and holds more generally for viscoelastic fluids in the limit of very small strain rates (Petrie, 2006). If $\zeta/\eta = K/G \Leftrightarrow \tau_B = \tau_S$ holds, one obtains $\tau_E = \tau_{B/S}$ as extensional retardation time constant (independent of ν).

Effective parameters modified by shear correction factors

It is well known that the stiffness parameters GA and GI_3 related to *shearing type* deformation modes systematically overestimate the actual stiffness of the structure for cross section geometries that display non–negligible warping.

In the case of transverse shearing, this is accounted for via a modification of the corresponding stiffness parameter $GA \rightarrow GA_\alpha := GA\varkappa_\alpha$ by introducing dimensionless *shear correction factors* $\varkappa_\alpha \leq 1$ depending on the cross section geometry (see Cowper, 1966; Gruttmann and Wagner, 2001). Likewise, the *torsional rigidity* $C_T = GJ_T$ of a rod exactly equals GI_3 in the case of (annular) circular cross sections only, but is smaller than this value otherwise due to the presence of out–of–plane warping of cross sections. The replacement $GI_3 \rightarrow C_T$ correcting this deficieny corresponds to the introduction of another dimensionless correction factor $\varkappa_3 = J_T/I_3 \leq 1$ depending on the cross section geometry[2] which modifies the torsional stiffness according to the replacement rule $GI_3 \rightarrow GJ_T = GI_3\varkappa_3$.

---

[2]In the case of an *elliptic* cross section with half axes a and b, the area moments are given by $I_1 = \frac{\pi}{4}a^3b$ and $I_2 = \frac{\pi}{4}ab^3$, while $C_T/G = J_T = \pi a^3b^3/(a^2+b^2) = 4I_1I_2/(I_1+I_2)$,

Altogether the various shear corrections mentioned above yield the corrected set of stiffness parameter values[3]

$$\hat{\mathbb{C}}_F \;=\; \mathrm{diag}\,(GA_1, GA_2, EA) \;\;,\;\; \hat{\mathbb{C}}_M \;=\; \mathrm{diag}\,(EI_1, EI_2, GJ_T) \;. \qquad (7)$$

We argue that the analogously modified damping parameters

$$\gamma_{S1/2} \;=\; GA_{1/2}\,\tau_S \;,\;\; \gamma_T \;=\; GJ_T\,\tau_S \qquad\qquad (8)$$

associated to shearing type rod deformations likewise provide a corresponding improvement of the formulas (6), which accounts for the influence of cross section warping on effective viscous dissipation, such that the *effective viscosity matrices* $\hat{\mathbb{V}}_F$ and $\hat{\mathbb{V}}_M$ introduced in (3) may be rewritten as

$$\hat{\mathbb{V}}_F \;=\; \hat{\mathbb{C}}_F \cdot \mathrm{diag}\,(\tau_S, \tau_S, \tau_E) \;\;,\;\; \hat{\mathbb{V}}_M \;=\; \hat{\mathbb{C}}_M \cdot \mathrm{diag}\,(\tau_E, \tau_E, \tau_S) \qquad (9)$$

in terms of the effective stiffness matrices and retardation time constants given above. A compact summary of our Kelvin–Voigt constitutive model for Cosserat rods is given in Fig. 1.

1.3 Related work on viscoelastic rods

While there is a rather large number of articles considering various kinds of damping terms (also of Kelvin–Voigt type) added to *linear* Euler–Bernoulli or Timoshenko beam models (usually assumed to have a straight reference geometry), one hardly finds any work on viscous damping models for *geometrically nonlinear* beams or rods in the literature.
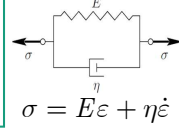
One notable exception is Antman's work (2003), where a damping model as given by eqns. (1) with positive, but otherwise undetermined parameters (3) is suggested from a completely different, mathematically motivated viewpoint, namely: as a simple possibility to introduce dissipative terms (denoted as *artificial viscosity*) into the dynamic balance equations of a Cosserat rod, which constitute a nonlinear coupled hyperbolic system of PDEs (see also

---

such that $\varkappa_3 = J_T/I_3 = 4I_1 I_2/(I_1+I_2)^2 \leq 1$ in this case. Equality ($\varkappa_3 = 1$) holds in the case of a circular cross section with $a = b = r \Rightarrow I_{1/2} = \frac{\pi}{4}r^4 = \frac{1}{2}I_3$ only. According to *Nikolai's inequality* $C_T \leq 4GI_1 I_2/(I_1+I_2)$ the special case of an elliptic cross section maximizes torsional rigidity among all asymmetric cross section geometries, and the value $GI_3 = 2GI$ valid for circular cross sections provides the absolute maximum of torsional rigidity (Berdichevsky, 1981).

[3]The stiffness parameters EA and EI_α are not affected by shear warping effects. However, they already account for *uniform lateral contraction*, which is a simple specific type of *in plane* cross section warping. This topic is discussed further in subsection 3.4 below.

KV type constitutive law for material stress resultants & couples:

$$\mathbf{F} = \hat{\mathbb{C}}_F \cdot (\mathbf{V} - \mathbf{V}_0) + \hat{\mathbb{V}}_F \cdot \partial_t \mathbf{V} = \hat{\mathbf{R}}^T \cdot \mathbf{f}\,,$$
$$\mathbf{M} = \hat{\mathbb{C}}_M \cdot (\mathbf{U} - \mathbf{U}_0) + \hat{\mathbb{V}}_M \cdot \partial_t \mathbf{U} = \hat{\mathbf{R}}^T \cdot \mathbf{m}$$

$$\sigma = E\varepsilon + \eta\dot{\varepsilon}$$

Effective stiffness matrices:

$$\hat{\mathbb{C}}_F = \mathrm{diag}\,(GA_1, GA_2, EA),\ \hat{\mathbb{C}}_M = \mathrm{diag}\,(EI_1, EI_2, GJ_T)$$

Elastic material parameters: **shear modulus G, Young's modulus E**
→ *Poisson's ratio*: $\nu = E/(2G) - 1$, *bulk modulus*: $3K = E/(1 - 2\nu)$

Effective viscosity matrices:

$$\hat{\mathbb{V}}_F = \mathrm{diag}\,(\eta A_1, \eta A_2, \eta_E A) = \hat{\mathbb{C}}_F \cdot \mathrm{diag}\,(\tau_S, \tau_S, \tau_E)$$
$$\hat{\mathbb{V}}_M = \mathrm{diag}\,(\eta_E I_1, \eta_E I_2, \eta J_T) = \hat{\mathbb{C}}_M \cdot \mathrm{diag}\,(\tau_E, \tau_E, \tau_S)$$

Viscous mat. param.: **shear viscosity** $\eta = G\tau_S$, bulk viscosity $\zeta = K\tau_B$

Extensional viscosity: $\eta_E = \zeta(1 - 2\nu)^2 + \frac{4}{3}\eta(1 + \nu)^2 = E\,\tau_E$

<u>*Note:*</u> Incompressible limit $\nu \to \frac{1}{2} \Rightarrow$ *Trouton's ratio* $\eta_E / \eta = \mathbf{3}$

Figure 1: Summary of the Kelvin–Voigt model for Cosserat rods.

Weiss, 2002a), and thereby achieve a *regularization* effect in view of the possible formation of shock waves that might appear in the *undamped* hyperbolic equations.

The recent article of Abdel–Nasser and Shabana (2011) is another relevant work for our topic. By inserting a 3D Kelvin–Voigt model into a geometrically nonlinear beam given in *absolute nodal coordinate formulation* (ANCF), the authors obtain a viscous damping model for such ANCF beams which (by construction) is closely related, but conceptually quite different from our approach proposed for Cosserat rods. Later we briefly discuss the relation of both damping models (see section 4.3). We refer othwise to the article of Romero (2008) for a comparison of the geometrically exact and ANCF approaches to nonlinear rods.

Mata, Oller and Barbat (2008) model the inelastic constitutive behaviour of composite beam structures under dynamic loading, using a Cosserat model as kinematical basis. However, they evaluate inelastic stresses by *numerical integration* of 3D Piola–Kirchhoff stresses *over 2D discretizations of the local cross sections* to obtain the stress resultants and couples of Simo's model.

6

This differs from our approach aiming at a *direct* formulation of frame–indifferent inelastic constitutive laws in terms of $\mathbf{F}$ and $\mathbf{M}$, as achieved e.g. by Simo et al. (1984) for viscoplastic rods. The viscous model proposed in section 3.2 of their paper is likewise of Kelvin–Voigt (KV) type, but formulated in terms of a vectorial strain measure related to the *Biot strain* (see also section A.2) and defined *pointwise* within the cross section. Moreover, they set up their model using only a *single* viscosity parameter.

Although there seems to be no further work on viscoelastic Cosserat rods made from solid material, *viscoelastic flow* in domains with rod–like geometries has been discussed in a number of articles. In his work on the coiling of viscous jets, Ribe (2004) presents a reduction of the three-dimensional Navier–Stokes equations to the dynamic equilibrium equations of a Kirchhoff/Love rod, endowed with Maxwell type constitutive equations for the viscous forces and moments which govern the finite resistance of the jet axis to stretching, bending and twisting. Although the derivation approach is different from ours, it represents its fluid–mechanical counterpart, as it likewise provides effective damping parameters[4] as given in (4), in the special case of an incompressible viscous fluid ($\nu = \frac{1}{2}$) with extensional viscosity given by Trouton's relation $\eta_E = 3\eta$, which in turn confirms our derivation of this special result.

A systematic derivation and mathematical investigation of viscous string and rod models in the context of Ribe's work is given by Panda et al. (2008) and Marheineke and Wegener (2009). Klar et al. (2009) and Arne et al. (2011) likewise use Ribe's Maxwell type constitutive law in their related work on the simulation of viscous fibers aiming at applications in the area of textile and nonwoven production. Lorenz et al. (2012) extend constitutive modelling for viscous strings by deriving an *upper convected Maxwell* model using mathematical methods of asymptotic analysis.

In the same context we finally mention the discrete modelling approach for viscous threads presented by Bergou et al. (2010), which extends earlier work of Bergou et al. (2008) on discrete elastic rods that, similar to our own approach as briefly presented in Linn et al. (2008) (see also Jung et al., 2011), relies on geometrically exact rod kinematics based on the *discrete differential geometry* of framed curves.

---

[4]In the case of viscous flow in a rod-shaped domain, the area $A(s)$ of the (circular) cross section as well as its geometric area moment $I(s)$ vary along the centerline curve in accordance with mass conservation modeled by a divergence-free velocity field of an extensional flow with uniform lateral contraction.

1.4   Overview of the remaining sections of the paper

After collecting a few basics of Cosserat rod theory in the following section 2, we proceed with our derivation of the formulas (4) in of a two–step procedure: In section 3 we start with the derivation of the elastic (*stored*) energy function

$$W_e(t) \;\; = \;\; \int_0^L ds \, \frac{1}{2} \Big[\Delta\mathbf{V}(s,t)^T \cdot \hat{\mathbb{C}}_F \cdot \Delta\mathbf{V}(s,t) \tag{10}$$
$$+ \;\; \Delta\mathbf{U}(s,t)^T \cdot \hat{\mathbb{C}}_M \cdot \Delta\mathbf{U}(s,t) \Big]$$

of a Cosserat rod, which is a quadratic functional of the terms $\Delta\mathbf{U}(s,t) = \mathbf{U}(s,t) - \mathbf{U}_0(s)$ and $\Delta\mathbf{V}(s,t) = \mathbf{V}(s,t) - \mathbf{V}_0(s)$ measuring the *change of the strain measures* w.r.t their reference values, from three-dimensional continuum theory.

This sets the notational and conceptional framework for the subsequent derivation of the viscous part of our damping model given in section 4 by an analogous procedure, which yields the *dissipation function*

$$D_v \;\; = \;\; \int_0^L ds \, \frac{1}{2} \Big[\partial_t\mathbf{V}^T \cdot \hat{\mathbb{V}}_F \cdot \partial_t\mathbf{V} \;\; + \;\; \partial_t\mathbf{U}^T \cdot \hat{\mathbb{V}}_M \cdot \partial_t\mathbf{U} \Big] \tag{11}$$

of a Cosserat rod introduced[5] in (Lang et al., 2011). The dissipation function (11), deduced from the three–dimensional (volumetric) continuum version of the dissipation function of a *Kelvin–Voigt solid* (Landau and Lifshitz, 1986; Lemaitre and Chaboche, 1990), corresponds to one half of the volume–integrated *viscous stress power* of a rod–shaped Kelvin–Voigt solid, such that $2D_v$ yields the rate at which the rod dissipates mechanical energy.

Having completed our derivation of the Kelvin–Voigt model, we proceed by a discussion of a seemingly straightforward, but, as it turns out, erroneous approach to derive the viscous parts of the forces and moments as given by (1) as resultants in analogy to the elastic counterparts. This shows that our energy–based approach to derive viscous damping is the proper one. After that, we briefly comment on the relation of our continuum model to the Kelvin–Voigt type model recently proposed by Abdel–Nasser and Shabana (2011) within their alternative ANCF approach to geometrically nonlinear rods, and conclude section 4 by a short discussion of the validity of the Kelvin–Voigt model w.r.t. a more general viscoelastic model of generalized Maxwell type.

---

[5]In (Lang et al., 2011) we absorbed the prefactor 1/2 into the definition (3) of the damping parameters (see eqns. (9) and (10) in sec. 2.2). This leads to an additional factor of 2 multiplying $\mathbb{V}_F$ and $\mathbb{V}_M$ in the constitutive equations (1) of the rod model.

Configuration variables:
- centerline curve: $\boldsymbol{\varphi} : [0,L] \times \mathbb{R} \to \mathbb{R}^3$
- moving frame: $\hat{\mathbf{R}}(s,t) = \mathbf{a}^{(k)}(s,t) \otimes \mathbf{e}_k \in SO(3)$
- curve parameter: $s \in [0,L]$, time: $t \in \mathbb{R}$
- cross section coordinates: $(\xi_1, \xi_2) \in A_0 \subset \mathbb{R}^2$

Current (deformed) configuration:
$$\mathbf{x}(\xi_1, \xi_2, s, t) = \boldsymbol{\varphi}(s,t) + \xi_\alpha \mathbf{a}^{(\alpha)}(s,t)$$

Reference configuration:
$$\mathbf{X}(\xi_1, \xi_2, s) = \boldsymbol{\varphi}_0(s) + \xi_\alpha \mathbf{a}_0^{(\alpha)}(s)$$
$$\partial_s \boldsymbol{\varphi}_0(s) = \mathbf{a}_0^{(3)}(s)$$
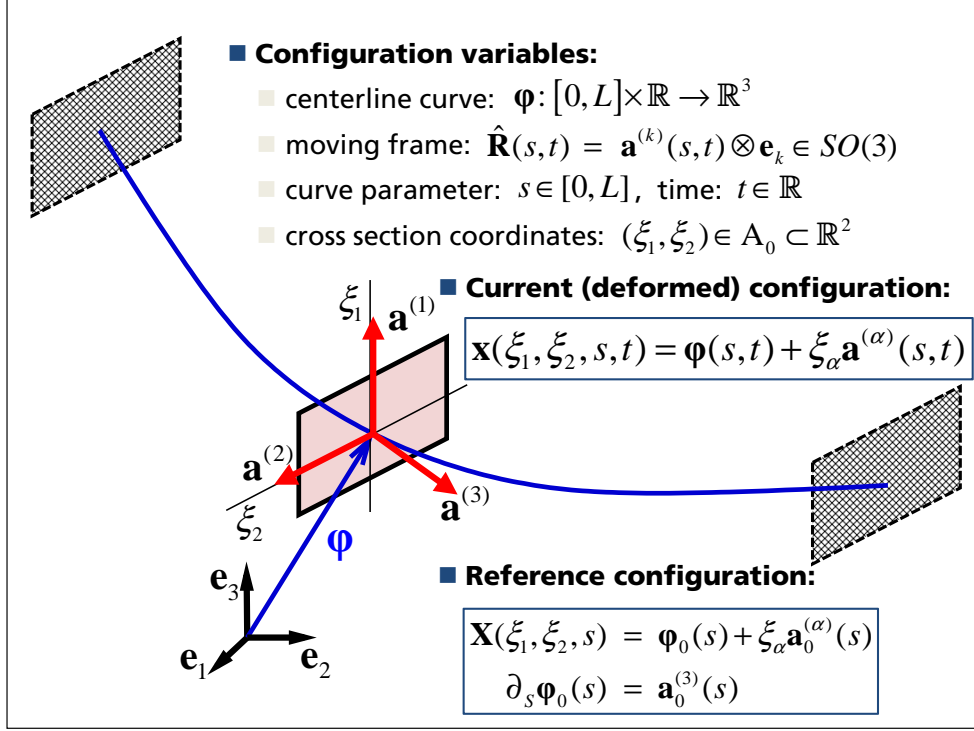
Figure 2: Kinematic quantities for the (deformed) current and (undeformed) reference configurations of a Cosserat rod.

In section 5, we illustrate the behaviour of our viscous damping model (1) by some simple numerical experiments with a clamped cantilever beam subject to bending with large deflections. We conclude our article with a short summary.

2 Basic Cosserat rod theory

The configuration variables of a Cosserat rod (see Antman, 2005) are its *centerline* curve $\boldsymbol{\varphi}(s,t) = \varphi_k(s,t)\,\mathbf{e}_k$ with cartesian component functions $\varphi_k(s,t)$ w.r.t. the fixed global ONB $\{\mathbf{e}_1, \mathbf{e}_2, \mathbf{e}_3\}$ of Euclidian space and *"moving frame"* $\hat{\mathbf{R}}(s,t) = \mathbf{a}^{(k)}(s,t) \otimes \mathbf{e}_k \in \mathsf{SO}(3)$ of orthonormal director vectors, both smooth functions of the curve parameter s and the time t, with the pair $\{\mathbf{a}^{(1)}, \mathbf{a}^{(2)}\}$ of directors spanning the local cross sections with normals $\mathbf{a}^{(3)}$ along the rod (see Fig. 2).
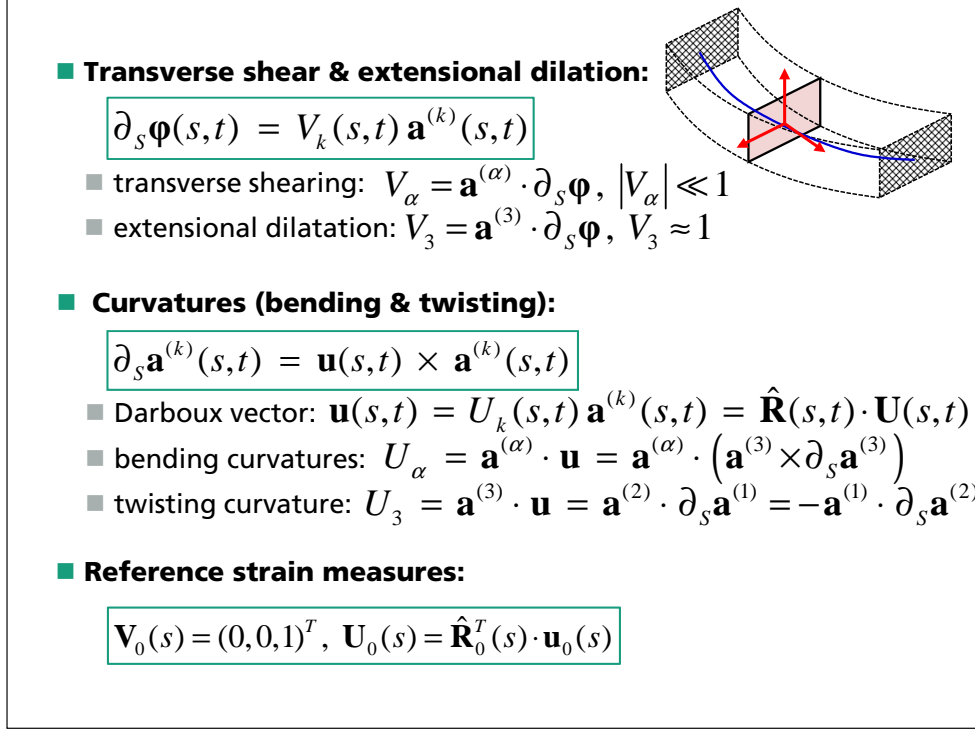
9

Transverse shear & extensional dilation:

$$\partial_s \boldsymbol{\varphi}(s,t) \;=\; V_k(s,t)\,\mathbf{a}^{(k)}(s,t)$$

- transverse shearing: $V_\alpha = \mathbf{a}^{(\alpha)} \cdot \partial_s \boldsymbol{\varphi}$, $\left|V_\alpha\right| \ll 1$
- extensional dilatation: $V_3 = \mathbf{a}^{(3)} \cdot \partial_s \boldsymbol{\varphi}$, $V_3 \approx 1$

Curvatures (bending & twisting):

$$\partial_s \mathbf{a}^{(k)}(s,t) \;=\; \mathbf{u}(s,t) \times \mathbf{a}^{(k)}(s,t)$$

- Darboux vector: $\mathbf{u}(s,t) \;=\; U_k(s,t)\,\mathbf{a}^{(k)}(s,t) \;=\; \hat{\mathbf{R}}(s,t) \cdot \mathbf{U}(s,t)$
- bending curvatures: $U_\alpha \;=\; \mathbf{a}^{(\alpha)} \cdot \mathbf{u} \;=\; \mathbf{a}^{(\alpha)} \cdot \left(\mathbf{a}^{(3)} \times \partial_s \mathbf{a}^{(3)} \right)$
- twisting curvature: $U_3 \;=\; \mathbf{a}^{(3)} \cdot \mathbf{u} \;=\; \mathbf{a}^{(2)} \cdot \partial_s \mathbf{a}^{(1)} = -\mathbf{a}^{(1)} \cdot \partial_s \mathbf{a}^{(2)}$

Reference strain measures:

$$\mathbf{V}_0(s) = (0,0,1)^T, \;\; \mathbf{U}_0(s) = \hat{\mathbf{R}}_0^T(s) \cdot \mathbf{u}_0(s)$$

Figure 3: Strain measures of a Cosserat rod for transverse shearing, extensional dilatation, bending and twisting.

2.1 Material strain measures

The material strain measures associated to the configuration variables are given by *(i)* the components $V_k = \mathbf{a}^{(k)} \cdot \partial_s \boldsymbol{\varphi}$ of the tangent vector in the local frame (i.e.: $\mathbf{V} = \hat{\mathbf{R}}^T \cdot \partial_s \boldsymbol{\varphi} = V_k \mathbf{e}_k$), with V_1, V_2 measuring *transverse shear* deformation and V_3 measuring *extensional dilatation*, and *(ii)* the *material Darboux vector* $\mathbf{U} = \hat{\mathbf{R}}^T \cdot \mathbf{u} = U_k \mathbf{e}_k$, obtained from its spatial counterpart $\mathbf{u} = U_k \mathbf{a}^{(k)}$ governing the Frénet equations $\partial_s \mathbf{a}^{(k)} = \mathbf{u} \times \mathbf{a}^{(k)}$ of the frame directors, with U_1, U_2 measuring *bending curvature* w.r.t. the director axes $\{\mathbf{a}^{(1)}, \mathbf{a}^{(2)}\}$, and U_3 measuring *torsional twist* around the cross section normal.

In general, the *reference configuration* of the rod, given by its centerline $\boldsymbol{\varphi}_0(s)$ and frame $\hat{\mathbf{R}}_0(s) = \mathbf{a}_0^{(k)}(s) \otimes \mathbf{e}_k$, may have non–zero curvature and twist (i.e.: $\mathbf{U}_0 \neq \mathbf{0}$). However we may assume zero initial shear ($V_{01} = V_{02} = 0$), such that all cross sections of the reference configuration are orthogonal to the centerline tangent vector, which coincides with the cross section normal (i.e.: $\partial_s \boldsymbol{\varphi}_0 = \mathbf{a}_0^{(3)} \Rightarrow V_{03} = 1$) if we choose the *arc–length* of the reference centerline as curve parameter s.
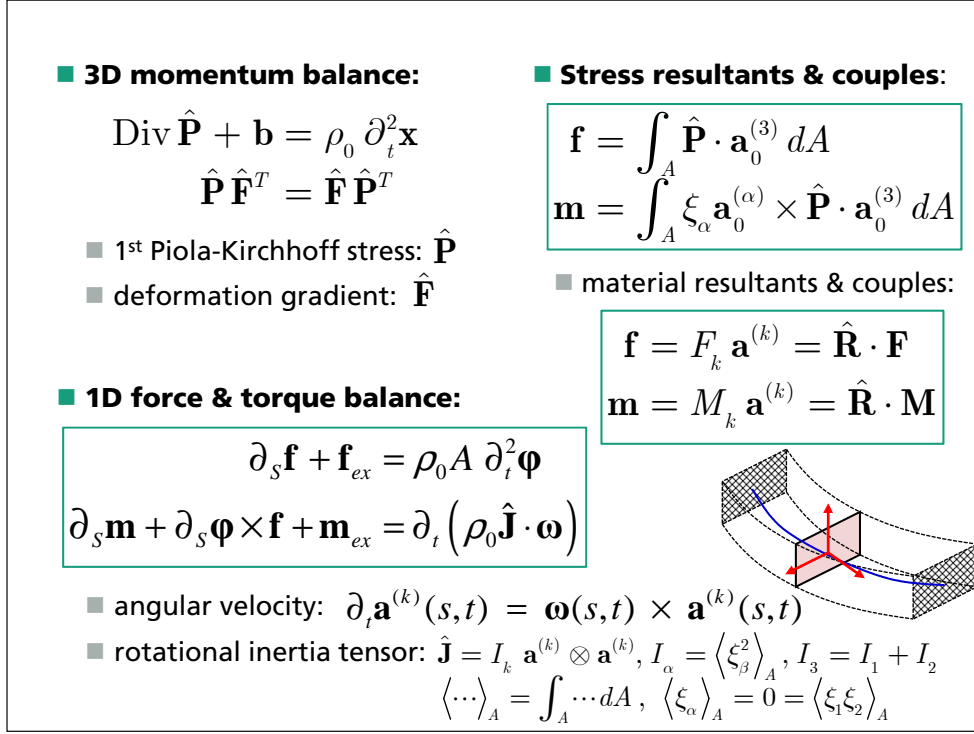
Figure 4: Dynamic equilibrium equations of a Cosserat rod.

2.2 Dynamic equilibrium equations

The constitutive equations (1) — or more general ones of viscoelastic type (see ch. 8.2 in Antman, 2005) — are required to close the system of dynamic equilibrium equations

$$\partial_s \mathbf{f} \; + \; \mathbf{f}_{ext} \;\; = \;\; (\rho_0 A)\, \partial_t^2 \boldsymbol{\varphi} \tag{12}$$

$$\partial_s \mathbf{m} \; + \; \partial_s \boldsymbol{\varphi} \times \mathbf{f} \; + \; \mathbf{m}_{ext} \;\; = \;\; \partial_t \left(\rho_0 \hat{\mathbf{J}} \cdot \boldsymbol{\omega} \right) \tag{13}$$

(see Fig. 4) which has to be satisfied by the *spatial* stress resultants $\mathbf{f} = \hat{\mathbf{R}} \cdot \mathbf{F}$ and stress couples $\mathbf{m} = \hat{\mathbf{R}} \cdot \mathbf{M}$ with appropriate boundary conditions (see Simo, 1985). The *inertial terms* appearing on the r.h.s. of the equations of the *balance of forces* (linear momentum) (12) and the *balance of moments* (angular momentum) (13) depend parametrically on the local *mass density* $\rho_0(s)$ along the rod as well as on geometrical parameters of the local cross section (area $A(s)$ and area moment tensor $\hat{\mathbf{J}}(s,t) = \hat{\mathbf{R}} \cdot \hat{\mathbf{J}}_0(s) \cdot \hat{\mathbf{R}}^T$) and contain the accelerations of the centerline positions $\partial_t^2 \boldsymbol{\varphi}(s,t)$ as well as the *angular velocity* vector $\boldsymbol{\omega}(s,t)$, which is implicitly defined by the the tem-

11

poral evolution equations $\partial_t \mathbf{a}^{(k)} = \boldsymbol{\omega} \times \mathbf{a}^{(k)}$ of the frame in close analogy to the Darboux vector, and its time derivative $\partial_t \boldsymbol{\omega}(s,t)$ as dynamical variables (see Simo (1985), Antman (2005) and Lang et al. (2011) for details).

Although we implemented Kelvin–Voigt type viscous damping given by (1) for our discrete[6] Cosserat model formulated with unit quaternions as explained in detail by Lang et al. (2011) and investigated further in (Lang and Arnold, 2012) w.r.t. numerical aspects, we do not make use of this particular formulation here, as it is more practical to work with the directors associated to $\mathsf{SO}(3)$ frames for the vector–algebraic calculations which we have to carry out within our derivations of one–dimensional rod functionals from three–dimensional continuum formulation.

2.3   Spatial configurations of a Cosserat rod

Introducing cartesian coordinates (ξ_1, ξ_2) w.r.t. the moving director basis $\{\mathbf{a}_0^{(1)}(s), \mathbf{a}_0^{(2)}(s)\}$ of the cross section located at the centerline point $\boldsymbol{\varphi}_0(s)$, the spatial positions of material points in the reference configuration of the rod are given by[7]

$$\mathbf{X}(\xi_1, \xi_2, s) \;=\; \boldsymbol{\varphi}_0(s) \,+\, \xi_\alpha \, \mathbf{a}_0^{(\alpha)}(s) \,. \tag{14}$$

As illustrated by Fig. 2, the positions of the same material points in the current (deformed) configuration are then given by

$$\mathbf{x}(\xi_1, \xi_2, s, t) \;=\; \boldsymbol{\varphi}(s,t) \,+\, \xi_\alpha \, \mathbf{a}^{(\alpha)}(s,t) \,+\, \mathbf{w}(\xi_1, \xi_2, s, t) \tag{15}$$

in terms of the deformed centerline curve $\boldsymbol{\varphi}(s,t)$, the rotated orthonormal cross section basis vectors $\{\mathbf{a}^{(1)}(s,t), \mathbf{a}^{(2)}(s,t)\}$, the same pair of cartesian cross section coordinates (ξ_1, ξ_2), and an additional displacement vector field $\mathbf{w}(\xi_1, \xi_2, s, t)$, which by definition describes the (in–plane and out–of–plane) *warping* deformations of the cross sections along the deformed rod.

The kinematic assumption that the cross sections of a rod remain *plane and rigid* in a configuration is equivalent to the assumption that the displacement field $\mathbf{w}$ vanishes identically. Although we will initially adhere to this

---

[6]Practical applications of our Cosserat rod model with Kelvin–Voigt damping in Multibody System Dynamics are reported in our recent collaboration with Schulze et al. (2012). We refer to the article of Zupan et al. (2009) for fundamental aspects of Cosserat rods with rotational d.o.f. represented by unit quaternions, as well as to the recent work (2012) of the same authors discussing the *undamped* dynamics of quaternionic Cosserat rods with various time integration approaches.

[7]Within this paper we make use of Einstein's summation convention — as the reader may have observed already — w.r.t. all indices occuring twice within *product* terms, with greek indices $\alpha, \beta, \ldots$ running from 1 to 2 and latin ones $i, j, k, \ldots$ from 1 to 3.

very common assumption for rod models, we will later admit some specific form of in–plane deformation of cross sections — namely: a *uniform lateral contraction* — to correct a deficiency w.r.t. artificial in–plane normal stresses caused by the excessively rigid kinematical ansatz (15) with $\mathbf{w} \equiv \mathbf{0}$.

For simplicity we assume the rod to be *prismatic*, such that all cross sections along the rod are identical, and the domain of the cartesian coordinates (ξ_1, ξ_2) coincides with one fixed domain $\mathcal{A} \subset \mathbb{R}^2$. As usual we choose the geometrical center of the domain $\mathcal{A}$ to coincide with the origin of $\mathbb{R}^2$ such that $\langle \xi_\alpha \rangle_{\mathcal{A}} = 0$ holds, where we introduced the shorthand notation $\langle f \rangle_{\mathcal{A}} := \int_{\mathcal{A}} f(\xi_1, \xi_2) \, d\xi_1 d\xi_2$ for the *cross section integral* of functions. In addition we choose the orientation of the orthonormal director pairs $\{\mathbf{a}_0^{(1)}(s), \mathbf{a}_0^{(2)}(s)\}$ as well as $\{\mathbf{a}^{(1)}(s,t), \mathbf{a}^{(2)}(s,t)\}$ to coincide with the principle geometrical axes of $\mathcal{A}$, such that $\langle \xi_1 \xi_2 \rangle_{\mathcal{A}} = 0$ holds. The quantities that characterize the geometric properties of the cross section in the Cosserat rod model are the *cross section area* $A = \langle 1 \rangle_{\mathcal{A}}$, the two *area moments* $I_1 = \langle \xi_2^2 \rangle_{\mathcal{A}}$, $I_2 = \langle \xi_1^2 \rangle_{\mathcal{A}}$ and the *polar area moment* $I_3 = \langle \xi_1^2 + \xi_2^2 \rangle_{\mathcal{A}} = I_1 + I_2$.

We obtain the centerline of the reference configuration as the average position $\boldsymbol{\varphi}_0(s) = \langle \mathbf{X} \rangle_{\mathcal{A}} / A$ of all material points of the cross section located at fixed s. The same relation $\boldsymbol{\varphi}(s,t) = \langle \mathbf{x} \rangle_{\mathcal{A}} / A$ holds for deformed configurations provided that the warping field $\mathbf{w}(\xi_1, \xi_2, s, t)$ satisfies $\langle \mathbf{w} \rangle_{\mathcal{A}} = \mathbf{0}$.

3 The stored energy of a Cosserat rod

In order to set the notational and conceptional framework for the derivation of the viscous part of our damping model, we first give a brief account of the derivation of its elastic part, i.e.: the stored energy function (10) of a Cosserat rod. Within this derivation we will encounter a variety of smallness assumptions w.r.t. the curvatures describing the reference geometry of the rod as well as the local strains occuring in its deformed configurations. In our subsequent derivation of the viscous dissipation function (11) we will use the same assumptions and thereby remain consistent with the derivation of the elastic part.

3.1 Three–dimensional strain measures

In the first step we compute the *deformation gradient* $\hat{\mathbf{F}} = \mathbf{g}_k \otimes \mathbf{G}^k$, the *right Cauchy–Green tensor* $\hat{\mathbf{C}} = \hat{\mathbf{F}}^T \cdot \hat{\mathbf{F}}$ and the *Green–Lagrange strain tensor* $\hat{\mathbf{E}} = \frac{1}{2}(\hat{\mathbf{C}} - \hat{\mathbf{I}})$ from the basis vectors $\mathbf{G}_k = \partial_k \mathbf{X}$ and $\mathbf{g}_k = \partial_k \mathbf{x}$ associated to the curvilinear coordinates of the rod configurations given by (14) and (15), with $\partial_k = \frac{\partial}{\partial \xi_k}$ for $k = 1, 2$ and $\partial_3 = \partial_s$ for $\xi_3 = s$.

The dual basis vectors $\mathbf{G}^j$ and $\mathbf{g}^j$ are defined by the relations $\mathbf{G}_i \cdot \mathbf{G}^j = \delta_{ij}$ and $\mathbf{g}_i \cdot \mathbf{g}^j = \delta_{ij}$ respectively. Proceeding in this way we obtain the basis vectors of the reference configuration (14) as $\mathbf{G}_\alpha = \mathbf{a}_0^{(\alpha)}(s)$ and $\mathbf{G}_3 = \mathbf{a}_0^{(3)}(s) + \xi_\alpha U_{0\alpha}(s)\mathbf{a}_0^{(\alpha)}(s)$. Their duals may be computed from the general formula $\mathbf{G}^i = \mathbf{G}_j \times \mathbf{G}_k / J_0$ with $J_0 := (\mathbf{G}_1 \times \mathbf{G}_2) \cdot \mathbf{G}_3$, where (ijk) is a cyclic permutation of the indices (123), with the result:

$\mathbf{G}^1 = \mathbf{a}_0^{(1)} + \xi_2 \frac{U_{03}}{J_0}\mathbf{a}_0^{(3)}$, $\mathbf{G}^2 = \mathbf{a}_0^{(2)} - \xi_1 \frac{U_{03}}{J_0}\mathbf{a}_0^{(3)}$, and $\mathbf{G}^3 = \frac{1}{J_0}\mathbf{a}_0^{(3)}$.

The inital curvatures $U_{0\alpha}(s)$ contained in the determinant $J_0(s) = 1 + \xi_2 U_{01}(s) - \xi_1 U_{02}(s)$ and the initial twist $U_{03}(s)$ of the reference configuration (14) influence the deviation of the dual vectors $\mathbf{G}^k$ from the frame directors $\mathbf{a}_0^{(k)}(s)$ within the cross section. Both vectors coincide if the reference configuration of the rod is straight and untwisted (i.e.: $\mathbf{U}_0 = \mathbf{0}$). We have approximate coincidence $\mathbf{G}^k \approx \mathbf{a}_0^{(k)}(s)$ if curvature and twist of the reference configuration are sufficiently weak, in the sense that for the curvature radii given by $R_k = 1/|U_{0k}|$ the estimates $|\xi_\alpha|/R_3 \ll 1$ and $|\xi_\alpha|/R_\beta \ll 1 \Rightarrow J_0 \approx 1$ hold throughout each cross section along the rod, such that all initial curvature radii R_α are large compared to the cross section diameter.

The geometric approximation $J_0(s) \approx 1$ will occur repeatedly and therefore play an important role in the derivation of the elastic energy and dissipation function of a Cosserat rod. To compute the deformation gradient we also need the basis vectors $\mathbf{g}_\alpha = \mathbf{a}^{(\alpha)}(s,t)$ and $\mathbf{g}_3 = \mathbf{a}^{(3)}(s,t) + \xi_\alpha U_\alpha(s,t)\mathbf{a}^{(\alpha)}(s,t)$ of the deformed configuration (15) with vanishing gradient of the warping vector field ($\partial_k \mathbf{w} = \mathbf{0}$). For the dual vectors $\mathbf{g}^k$ one obtaines analogous expressions as those for the dual vectors $\mathbf{G}^k$ given above, which we omit here.

For the special kinematical relations of a Cosserat rod, the deformation gradient $\hat{\mathbf{F}} = \mathbf{g}_k \otimes \mathbf{G}^k$ may be expressed in terms of a *pseudo–polar decomposition* (see Géradin and Cardona, 2001) by a factorization of the *relative rotation* $\hat{\mathbf{R}}_{rel}(s,t) := \hat{\mathbf{R}}(s,t) \cdot \hat{\mathbf{R}}_0^T(s) = \mathbf{a}^{(k)}(s,t) \otimes \mathbf{a}_0^{(k)}(s)$ connecting the moving frames of the reference and deformed configurations of the rod. The resulting formula

$$\hat{\mathbf{F}}(\xi_1, \xi_2, s, t) = \hat{\mathbf{R}}_{rel}(s,t) \left[\hat{\mathbf{I}} + \frac{1}{J_0(s)} \mathbf{H}(\xi_1, \xi_2, s, t) \otimes \mathbf{a}_0^{(3)}(s) \right] \qquad (16)$$

depends on the *absolute values* of the curvatures of the reference configuration (14) through $J_0(s)$, and on the *change of the strain measures* of the rod given by the difference vectors $\mathbf{U}(s,t) - \mathbf{U}_0(s)$ and $\mathbf{V}(s,t) - \mathbf{V}_0$ with $\mathbf{V}_0 = (0,0,1)^T$ in terms of the *material strain vector* $\mathbf{H}(\xi_1, \xi_2, s, t) = H_k(\xi_1, \xi_2, s, t)\mathbf{a}_0^{(k)}(s)$

with components

$$
\begin{aligned}
H_1(\xi_2, s, t) &= V_1(s, t) - \xi_2 \left[U_3(s, t) - U_{03}(s) \right] , \\
H_2(\xi_1, s, t) &= V_2(s, t) + \xi_1 \left[U_3(s, t) - U_{03}(s) \right] , \\
H_3(\xi_1, \xi_2, s, t) &= \left[V_3(s, t) - 1 \right] + \xi_2 \left[U_1(s, t) - U_{01}(s) \right] \\
&\quad - \xi_1 \left[U_2(s, t) - U_{02}(s) \right] ,
\end{aligned}
\tag{17}
$$

which can be written more compactly[8] in the form of a cartesian vector $\hat{\mathbf{R}}_0^T \cdot \mathbf{H} = (\mathbf{V} - \mathbf{V}_0) - \xi_\alpha \mathbf{e}_\alpha \times (\mathbf{U} - \mathbf{U}_0) = H_k \mathbf{e}_k$ w.r.t. the fixed global frame.

Computing the right Cauchy–Green tensor $\hat{\mathbf{C}} = \hat{\mathbf{F}}^T \cdot \hat{\mathbf{F}}$ with the deformation gradient given by (16) results in the following exact expression for the Green–Lagrange strain tensor:

$$
\hat{\mathbf{E}} = \frac{1}{2J_0} \left[\mathbf{H} \otimes \mathbf{a}_0^{(3)} + \mathbf{a}_0^{(3)} \otimes \mathbf{H} \right] + \frac{\mathbf{H}^2}{2J_0^2} \mathbf{a}_0^{(3)} \otimes \mathbf{a}_0^{(3)} .
\tag{18}
$$

The approximate expression[9]

$$
\hat{\mathbf{E}} \approx \frac{1}{2} \left[\mathbf{H} \otimes \mathbf{a}_0^{(3)} + \mathbf{a}_0^{(3)} \otimes \mathbf{H} \right]
\tag{19}
$$

may be obtained from (18) by the geometric approximation $J_0 \approx 1$ assumed to hold for the reference geometry and the additional assumption $\|\mathbf{H}\| \ll 1$ of a *small material strain vector*.

Later we will make use of the approximate strain tensor (19), which is *linear* in the vector field $\mathbf{H}$ and therefore also in the change of the strain measures of the rod, to obtain the stored energy function (10), which then becomes a *quadratic form* in the change of the strain measures. Likewise we will use (19) to obtain an approximation of the strain rate $\partial_t \mathbf{E}$ in terms of the rate $\partial_t \mathbf{H}$ of the strain vector.

---

[8]Our derivation generalizes the one given by Géradin and Cardona (2001) for the simpler case of a straight and untwisted reference configuration of the rod (i.e. $\mathbf{U}_0 = 0$). Apart from using a slightly different and more compact notation, the kinematically exact expression of the deformation gradient given by eqns. (16) and (17) is algebraically equivalent to the one given by Kapania and Li (2003) in eq. (47) of their paper. We note that the difference terms $\mathbf{U} - \mathbf{U}_0$ and $\mathbf{V} - \mathbf{V}_0$ appear already in the kinematically exact expression (18) *before* discarding second order terms. This shows that our approach is more general than the one chosen by Weiss (2002a).

[9]We note that (19) may alternatively be interpreted as an *approximation of the Biot strain* (see section A.1 of the appendix).

3.2 Validity of the small strain approximation

For deformed configurations of a slender rod one observes large displacements and rotations, but local strains remain small. To estimate the size of the strain tensor it is useful to compute its components $E_{ij} = \mathbf{a}_0^{(i)} \cdot (\hat{\mathbf{E}} \cdot \mathbf{a}_0^{(j)})$ w.r.t. the tensor basis $\mathbf{a}_0^{(i)} \otimes \mathbf{a}_0^{(j)}$ obtained from the directors of the reference frame $\hat{\mathbf{R}}_0(s)$. From (18) and (19) we obtain identically vanishing in–plane components ($E_{\alpha\beta} = E_{\beta\alpha} \equiv 0$), as well as the exact and approximate expressions

$$E_{\alpha 3} = E_{3\alpha} = \frac{H_\alpha}{2J_0} \approx \frac{H_\alpha}{2} \; , \quad E_{33} = \frac{H_3}{J_0} + \frac{\mathbf{H}^2}{2J_0^2} \approx H_3 \tag{20}$$

of the components related to out–of–plane deformations of the local cross section. Introducing the the quantity $|\xi|_{max} := \max_{(\xi_1,\xi_2)\in\mathcal{A}}(|\xi_1|, |\xi_2|)$ to estimate the maximal linear extension of the cross section $\mathcal{A}$, one may estimate the deviation of the determinant $J_0(s)$ from unity by $|J_0(s) - 1| \leq |\xi|_{max}(1/R_1 + 1/R_2)$ as a coarse check of the validity of the approximation $J_0 \approx 1$. Otherwise the smallness of the components of $\hat{\mathbf{E}}$ is implied by the smallness of the components H_k of the strain vector. According to (17) these components in turn become small if the change of the strain measures of the Cosserat rod is small, i.e. if the estimates $|V_\alpha| \ll 1$, $|V_3 - 1| \ll 1$, $|U_k - U_{0k}| \ll 1/|\xi|_{max}$ hold.

For slender rods with moderately curved undeformed geometry these estimates are obviously easily satisfiable, except for extreme deformations of the rod that produce large curvatures or twists of the order of the inverse cross section diameter. In this case, the assumption of small strains obviously would be invalid.

3.3 Elastic constitutive behaviour at small strains

If we assume the rod material to behave hyperelastically with a stored energy density function $\Psi_e(\hat{\mathbf{E}})$, a simple Taylor expansion argument[10] shows that the behaviour of the energy density within the range of small strains may be well approximated by the quadratic function $\Psi_e(\hat{\mathbf{E}}) \approx \frac{1}{2}\hat{\mathbf{E}} : \mathbb{H} : \hat{\mathbf{E}}$, where $\mathbb{H} = \partial_{\hat{\mathbf{E}}}^2 \Psi_e(\hat{\mathbf{0}})$ is the fourth order *Hookean material tensor* known from linear elasticity. This quadratic approximation yields a well defined frame–indifferent elastic energy density that is suitable for structure deformations at small local strains, but arbitrary large displacements and rotations, and

---

[10]Additional assumptions are the vanishing of the elastic energy density at zero strain ($\Psi_e(\hat{\mathbf{0}}) = 0$), as well as the absence of initial stresses in the undeformed configuration (i.e.: $\hat{\mathbf{S}}_0 = \partial_{\hat{\mathbf{E}}}\Psi_e(\hat{\mathbf{0}}) = \hat{\mathbf{0}}$).

therefore serves as a proper basis for the derivation of the stored energy function of a Cosserat rod.

The corresponding approximation of the stress–strain relation yields the 2nd *Piola–Kirchhoff stress* tensor $\hat{\mathbf{S}} = \partial_{\hat{\mathbf{E}}}\Psi_e(\hat{\mathbf{E}}) \approx \mathbb{H} : \hat{\mathbf{E}}$ for small strains. The 1st *Piola–Kirchhoff stress* tensor $\hat{\mathbf{P}}$, which is used to define the stress resultants and stress couples of the Cosserat rod model (see Simo, 1985, for details), is obtained by the transformation $\hat{\mathbf{P}} = \hat{\mathbf{F}} \cdot \hat{\mathbf{S}}$ using the deformation gradient, and the Cauchy stress tensor as the inverse Piola transformation $\hat{\boldsymbol{\sigma}} = J^{-1}\hat{\mathbf{P}} \cdot \hat{\mathbf{F}}^T$ depending also on $J = \det(\hat{\mathbf{F}})$. If we approximate the strain tensor $\hat{\mathbf{E}}$ by (19) and consistently discard all terms that are of second order in $\|\mathbf{H}\|$ in accordance with our assumption of small strains, we have to use the approximation $\hat{\mathbf{F}} \approx \hat{\mathbf{R}}_{rel}(s)$ (which implies $J \approx 1$) for the deformation gradient in all stress tensor transformations. This means that all pull back or push forward transformations are carried out approximately as simple relative rotations connecting corresponding frames $\hat{\mathbf{R}}_0(s)$ and $\hat{\mathbf{R}}(s,t)$ of the undeformed and deformed configurations of a Cosserat rod. Alltogether we obtain the approximate expressions[11]

$$\hat{\mathbf{S}} \approx \mathbb{H} : \hat{\mathbf{E}} \;\;\Rightarrow\;\; \hat{\mathbf{P}} \approx \hat{\mathbf{R}}_{rel} \cdot \hat{\mathbf{S}}\,, \;\; \hat{\boldsymbol{\sigma}} \approx \hat{\mathbf{R}}_{rel} \cdot \hat{\mathbf{S}} \cdot \hat{\mathbf{R}}_{rel}^T \qquad (21)$$

for the various stress tensors, which are valid for the specific type of small strain assumptions encountered for Cosserat rods, as discussed above.

In the case of a *homogeneous and isotropic* material, the Hookean tensor acquires the special form of an isotropic fourth order tensor $\mathbb{H}_{SVK} = \lambda \hat{\mathbf{I}} \otimes \hat{\mathbf{I}} + 2\mu \mathbb{I}$ depending on two constant elastic moduli: the *Lamé parameters* λ and μ. Here $\hat{\mathbf{I}}$ and $\mathbb{I}$ are the second and fourth order identity tensors, which act on (symmetric) second order tensors $\hat{\mathbf{Q}}$ by double contraction as $\mathbb{I} : \hat{\mathbf{Q}} = \hat{\mathbf{Q}}$ and $\hat{\mathbf{I}} : \hat{\mathbf{Q}} = \text{Tr}(\hat{\mathbf{Q}})$, such that one obtains $\hat{\mathbf{Q}} : (\hat{\mathbf{I}} \otimes \hat{\mathbf{I}}) : \hat{\mathbf{Q}} = \text{Tr}(\hat{\mathbf{Q}})^2$ and $\hat{\mathbf{Q}} : \mathbb{I} : \hat{\mathbf{Q}} = \hat{\mathbf{Q}} : \hat{\mathbf{Q}} = \text{Tr}(\hat{\mathbf{Q}}^2) = \|\hat{\mathbf{Q}}\|_F^2$, where $\| \ldots \|_F$ is the Frobenius norm. The corresponding energy function is the *Saint–Venant Kirchhoff* potential

$$\begin{aligned}\Psi_{SVK}(\hat{\mathbf{E}}) &= \frac{1}{2}\,\hat{\mathbf{E}} : \mathbb{H}_{SVK} : \hat{\mathbf{E}} && (22)\\[4pt] &= \frac{\lambda}{2}\,\text{Tr}(\hat{\mathbf{E}})^2 \;+\; \mu\,\|\hat{\mathbf{E}}\|_F^2 \;=\; \frac{K}{2}\,\text{Tr}(\hat{\mathbf{E}})^2 \;+\; \mu\,\|\mathbb{P} : \hat{\mathbf{E}}\|_F^2\,,\end{aligned}$$

where $\mathbb{P} = \mathbb{I} - \frac{1}{3}\hat{\mathbf{I}} \otimes \hat{\mathbf{I}}$ is the orthogonal projector on the subspace of traceless second order tensors, such that $\mathbb{P} : \hat{\mathbf{E}} = \hat{\mathbf{E}} - \frac{1}{3}\text{Tr}(\hat{\mathbf{E}})\hat{\mathbf{I}}$ yields the traceless (deviatoric) part of the strain tensor, and $K = \lambda + \frac{2}{3}\mu$ is the bulk modulus.

---

[11]An alternative interpretation of (21) in terms of the Biot stress tensor is briefly discussed in section A.3 of the appendix.

3.4 Modified strain accounting for lateral contraction

The stress–strain relation obtained from (22) is given by

$$\hat{\mathbf{S}}_{SVK} \;=\; \lambda\,\mathrm{Tr}(\hat{\mathbf{E}})\,\hat{\mathbf{I}} \;+\; 2\mu\,\hat{\mathbf{E}} \;=\; K\,\mathrm{Tr}(\hat{\mathbf{E}})\,\hat{\mathbf{I}} \;+\; 2\mu\,\mathbb{P}:\hat{\mathbf{E}}\,. \qquad (23)$$

Inserting the approximate expressions (19) and (20) of the strain tensor and its components into (23) yields the small strain approximation $\hat{\mathbf{S}}_{SVK} \approx \lambda H_3\hat{\mathbf{I}} + \mu[\mathbf{H} \otimes \mathbf{a}_0^{(3)} + \mathbf{a}_0^{(3)} \otimes \mathbf{H}]$ of the stress tensor $\hat{\mathbf{S}}_{SVK}$ for Cosserat rods. The computation of the stress components w.r.t. the basis of $\hat{\mathbf{R}}_0(s)$ directors yields normal stress components $S_{\alpha\alpha} \approx \lambda H_3$ and $S_{33} \approx (\lambda + 2\mu)H_3$, and the shear stress components are given by $S_{12} = S_{21} = 0$ and $S_{\alpha3} = S_{3\alpha} \approx \mu H_\alpha$ respectively.

As both elastic moduli $\lambda = 2\mu\nu/(1-2\nu)$ and $\lambda+2\mu = 2\mu(1-\nu)/(1-2\nu)$ appearing in the expressions for the normal stress components, expressed in terms of the shear modulus $\mu = G$ and Poisson's ratio given by $2\nu = \lambda/(\lambda+\mu)$, diverge in the incompressible limit $\nu \to \frac{1}{2}$ (just as the bulk modulus $K = \frac{2}{3}\frac{1+\nu}{1-2\nu}G$ does), the normal stresses would become infinitely large whenever the normal strain $E_{33} \approx H_3$ becomes nonzero. This unphysical behaviour is a direct consequence of the kinematical assumption of plain and *rigid* cross section, which prevents any lateral contraction of the cross section in the case of a longitudinal extension. Therefore the assumption of a *perfectly rigid* cross section, as well as the expressions (18) and (19) derived under this assumption, are strictly compatible only with *perfectly compressible* materials (i.e.: in the special case $\nu = 0$).

The standard procedure to fix this deficiency (see e.g. Weiss, 2002a) is based on the plausible requirement that *all* in–plane stress components $S_{\alpha\beta}$ (including the normal stresses $S_{\alpha\alpha}$), which for rods in practice are very small compared to the out of plain normal and shear stresses $S_{\alpha3}$ and S_{33}, should *vanish* completely. This may be achieved by imposing a *uniform lateral contraction* with in–plane normal strain components $E_{\alpha\alpha} = -\nu E_{33}$ upon the cross section.

Although this procedure seems to be an ad hoc one, it may be justified by an asymptotic analysis[12] of the local strain field for rods, e.g. in the way as presented by A.E.H. Love (1927) in the paragraph §256 on the *"Nature of the strain in a bent and twisted rod"* in Ch. XVIII of his book. Following Love's analysis, we obtain the in–plane normal strains to leading order as $E_{\alpha\alpha} = \partial_\alpha w_\alpha = -\nu E_{33}$ with the additional requirement that $E_{12} = E_{21} = \partial_1 w_2 + \partial_2 w_1 = 0$, which determines the in–plane components w_α of the the warping field $\mathbf{w}$ corresponding to the lateral contraction in terms of E_{33}.

---

[12]See (Berdichevsky, 1981) and ch. 15 of (Berdichevsky, 2009) for a modern comprehensive analysis within Berdichevsky's variational asymptotic approach.

To obtain the modified value of $E_{\alpha\alpha} = -\nu E_{33}$ one has to add an additional term $-\nu E_{33}\, \mathbf{a}_0^{(\alpha)} \otimes \mathbf{a}_0^{(\alpha)}$ to the exact expression (18) of the strain tensor. Using the identity $\hat{\mathbf{I}} = \mathbf{a}_0^{(k)} \otimes \mathbf{a}_0^{(k)}$, we obtain the modified expression

$$\hat{\mathbf{E}}' \;=\; \hat{\mathbf{E}} \;-\; \nu\, E_{33} \left[\hat{\mathbf{I}} - \mathbf{a}_0^{(3)} \otimes \mathbf{a}_0^{(3)} \right] \tag{24}$$

for the strain tensor, with $E_{33} \approx H_3$ as small strain approximation according to (19). Inserting the modified strain tensor (24) into the stress–strain equation of the Saint–Venant–Kirchhoff material with $\mathrm{Tr}(\hat{\mathbf{E}}') = (1 - 2\nu)E_{33} \approx (1 - 2\nu)H_3$, and using the relation $\lambda(1 - 2\nu) = \frac{\nu}{1+\nu}E$ that relates the Lamé parameter λ to Young's modulus E, we obtain the following modified expression for the stress of a Cosserat rod:

$$\hat{\mathbf{S}}'_{SVK} \;\approx\; \frac{E\nu}{1 + \nu}\, H_3\, \mathbf{a}_0^{(3)} \otimes \mathbf{a}_0^{(3)} \;+\; G \left[\mathbf{H} \otimes \mathbf{a}_0^{(3)} + \mathbf{a}_0^{(3)} \otimes \mathbf{H} \right] \;. \tag{25}$$

By construction, we now obtain vanishing in–plane stress components $S'_{12} = S'_{21} = S'_{\alpha\alpha} \equiv 0$, while the transverse shear stresses remain unaffected by the modification (i.e.: $S'_{\alpha 3} = S'_{3\alpha} \approx G H_\alpha$ with $G = \mu$). As $2G = E/(1 + \nu)$, we likewise obtain the modified expression $S'_{33} \approx E\, H_3$ for the normal stress component orthogonal to the cross section, which corresponds to the familiar expression from elementary linear beam theory, with Young's modulus E replacing $\lambda + 2\mu$.

3.5 Elastic energy of a Cosserat rod

Next we demonstrate briefly how the modified expressions (24) and (25) directly lead to the well known stored energy function (10).

In the case of a hyperelastic material with an elastic (stored) energy density Ψ_e the elastic potential energy of a body is given by the volume integral $\int_{V_0} dV\, \Psi_e$ of the energy density over the volume V_0 of the reference configuration of the body. In the case of a rod shaped body parametrized by the coordinates (ξ_1, ξ_2, s) of the reference configuration (14), the volume measure of V_0 is given by $dV = J_0\, ds\, d\xi_1 d\xi_2$, where J_0 is the Jacobian of the reference configuration (see subsection 3.1). Using the geometric approximation $J_0 \approx 1$, the stored energy function of a rod shaped body is obtained as the integral $\int_{V_0} dV\, \Psi_e \approx \int_0^L ds\, \langle \Psi_e \rangle_{\mathcal{A}}$ of the density over the cross sections and along the centerline of the reference configuration of the rod.

In the special case of the energy density (22) this leads to the stored energy function $W_e = \int_0^L ds\, \left\langle \Psi_{SVK}(\hat{\mathbf{E}}') \right\rangle_{\mathcal{A}}$, using the modified strain tensor $\hat{\mathbf{E}}'$ from (24). Applying our previously introduced approximations of small

strains and small initial curvature, we obtain the approximate expression

$$\Psi_{SVK}(\hat{\mathbf{E}}') \;=\; \frac{1}{2}\hat{\mathbf{S}}'_{SVK}:\hat{\mathbf{E}}' \;\approx\; \frac{1}{2}\left[EH_3^2 \,+\, G(H_1^2 + H_2^2)\right] \qquad (26)$$

for the energy density. Its cross section integral $\left\langle \Psi_{SVK}(\hat{\mathbf{E}}') \right\rangle_{\mathcal{A}}$ may be evaluated in terms of the integrals

$$\begin{aligned}
\left\langle H_1^2 + H_2^2 \right\rangle_{\mathcal{A}} &= A(V_1^2 + V_2^2) \,+\, I_3(U_3 - U_{03})\,,\\
\left\langle H_3^2 \right\rangle_{\mathcal{A}} &= A(V_3 - 1)^2 \,+\, I_\alpha(U_\alpha - U_{0\alpha})\,,
\end{aligned}$$

which finally yields the desired result

$$\begin{aligned}
2\left\langle \Psi_{SVK}(\hat{\mathbf{E}}') \right\rangle_{\mathcal{A}} &\approx\; EA(V_3 - 1)^2 \,+\, GA(V_1^2 + V_2^2) \qquad (27)\\
&+\; EI_\alpha(U_\alpha - U_{0\alpha}) \,+\, GI_3(U_3 - U_{03})\,,
\end{aligned}$$

corresponding exactly to the stored energy function (10) with effective stiffness parameters given by (2). The subsequent introduction of *shear correction factors* $(GA \to GA\varkappa_\alpha)$ as well as the corresponding correction $GI_3 \to GJ_T = GI_3\varkappa_3$ of *torsional rigidity*[13] finally yields the stored energy function (10) with correspondingly modified effective stiffnesses as given by (7) (see also section 4.1 for a more detailed discussion of this point).

---

[13] The correction of torsional rigidity accounts for the contribution of out–of–plane cross section warping in terms of a corresponding torsional stress function $\Phi(\xi_1, \xi_2)$ and leads to an improved approximation of the strain and stress fields as well as the resulting elastic energy given by (10) compared to its 3D volumetric counterpart. Similar arguments apply to an improved approximation of transverse shear strains and stresses as well as the associated part of the elastic energy density by accounting for additional contributions given by a corresponding pair of stress functions $\chi_\alpha(\xi_1, \xi_2)$. The classical results obtained by St.–Venant are given in ch. XIV of Love's treatise (Love, 1927) (see also ch. II §16 in (Landau and Lifshitz, 1986)). They are contained as a special (and simplified) case within Berdichevsky's more comprehensive and modern treatment in terms of his method of variational asymptotic analysis applied to rods (see (Berdichevsky, 1981, 1983) and ch. 15 of (Berdichevsky, 2009)). Apart of Timoshenko's original treatment of shear correction factors, the article of Cowper (1966) is a classical reference on this subject, with correction factors obtained from pointwise (centroidal) and cross section averaged values of transverse shear stresses $\sigma_{\alpha3}$ (see also the discussions in ch. II, section 11. of Villagio (1997) and section 2.1 of Simo et al. (1984)). More recently an alternative approach based on *energy balance* as utilized e.g. in (Gruttmann and Wagner, 2001) and likewise fits to our considerations, is considered as standard due to superior results. However, the issue of correction factors for transverse shear in Timoshenko–type rod models is still subject of discussion and research activities (see e.g. Dong et al., 2010).

3.6 Kinetic energy and energy balance for rods

In general, the kinetic energy of a body is given by the volume integral $\int_{V_0} dV \frac{1}{2}\rho_0 \mathbf{v}^2$, where $\rho_0(\mathbf{X})$ is the local mass density of the body in the reference volume, and $\mathbf{v}(\mathbf{X}, t) = \partial_t \mathbf{x}(\mathbf{X}, t)$ is the velocity of the respective material point. Using the kinematic ansatz (15) with the geometric approximation $J_0 \approx 1$, assuming a homogeneous mass density, and neglecting the contribution of cross section warping ($\mathbf{w} \equiv 0$), we obtain the integral expression $W_k = \int_0^L ds \frac{1}{2}\rho_0[A(\partial_t \boldsymbol{\varphi})^2 + \langle \xi_\alpha^2 \rangle_{\mathcal{A}} (\partial_t \mathbf{a}^{(\alpha)})^2]$ for the kinetic energy of the rod as a quadratic functional of the time derivatives of its kinematic variables. The rotatory part may be reformulated in terms of the material components $\Omega_j = \boldsymbol{\omega} \cdot \mathbf{a}^{(j)}$ of the angular velocity vector $\boldsymbol{\omega} = \Omega_j \mathbf{a}^{(j)}$ of the rotating frame, which is implicitly defined by $\partial_t \mathbf{a}^{(k)} = \boldsymbol{\omega} \times \mathbf{a}^{(j)}$, by substituting $\langle \xi_\alpha^2 \rangle_{\mathcal{A}} (\partial_t \mathbf{a}^{(\alpha)})^2 = I_k \Omega_k^2$. This finally yields the familiar expression $W_k = \int_0^L ds \frac{1}{2}\rho_0[A(\partial_t \boldsymbol{\varphi})^2 + I_k \Omega_k^2]$ for the kinetic energy of a Cosserat rod as given in Lang et al. (2011) with Ω_k expressed in quaternionic formulation. Altogether we obtain the approximation $\int_{V_0} dV [\frac{1}{2}\rho_0 \mathbf{v}^2 + \Psi_e] \approx W_e + W_k =: W_m$ of the three–dimensional mechanical energy of a rod shaped body in terms of the corresponding sum of the kinetic and stored energy functions W_k and W_e of the Cosserat rod model as given above. In the absence of any dissipative effects, the mechanical energy must be conserved *exactly* in both the 3D as well as the 1D setting, such that the identities $\frac{d}{dt}\int_{V_0} dV [\frac{1}{2}\rho_0 \mathbf{v}^2 + \Psi_e] = 0 = \frac{d}{dt}W_m$ hold identically as a consequence of the respective balance equations for both the 3D volumetric body and the 1D rod.

4 Kelvin–Voigt damping for Cosserat rods

Now we have collected all technical prerequisites and approximate results that enable us to derive the dissipation function (11) of a Cosserat rod from a three-dimensional Kelvin–Voigt model in analogy to the derivation of the stored energy function (10) in a consistent way.

In Landau and Lifshitz (1986) (see Ch. V §34) the *dissipation function* $\int_V dV \frac{1}{2}\eta_{ijkl}\dot{\varepsilon}_{ij}\dot{\varepsilon}_{kl}$ is considered as an appropriate model of dissipative effects within a solid body near thermodynamic equilibrium, with constant fourth order tensor components η_{ijkl} that are the viscous analogon of the components of the Hookean elasticity tensor. According to our formulation, the dissipation function suggested by Landau and Lifshitz (1986) becomes that of a *Kelvin–Voigt* solid (see Lemaitre and Chaboche, 1990):

$$D_{KV} = \int_0^L ds \left\langle \Psi_{KV}(\partial_t \hat{\mathbf{E}}) \right\rangle_{\mathcal{A}} = \int_0^L ds \frac{1}{2} \left\langle \partial_t \hat{\mathbf{E}} : \mathbb{V} : \partial_t \hat{\mathbf{E}} \right\rangle_{\mathcal{A}} . \qquad (28)$$

This is a quadratic form in the material strain rate $\partial_t \hat{\mathbf{E}}$ defined as the time derivative of the Green–Lagrange strain tensor. The constant fourth order *viscosity tensor* $\mathbb{V}$ may be assumed to have the same symmetries as the Hookean tensor $\mathbb{H}$, depending on *viscosity parameters* in the same way as the components of $\mathbb{H}$ depend on elastic moduli. The stress–strain relation of the Kelvin–Voigt model is given by $\hat{\mathbf{S}} = \mathbb{H} : \hat{\mathbf{E}} + \mathbb{V} : \partial_t \hat{\mathbf{E}}$, with the viscous stress[14] given by the term $\hat{\mathbf{S}}_v := \mathbb{V} : \partial_t \hat{\mathbf{E}} = \partial_{\partial_t \hat{\mathbf{E}}} \Psi_{KV}(\partial_t \hat{\mathbf{E}})$.

The dissipation function for a Cosserat rod results by inserting the rate $\partial_t \hat{\mathbf{E}}'$ of the modified strain tensor (24) into the dissipation density function Ψ_{KV} of the Kelvin–Voigt model. We will compute this function explicitly in closed form for the special case of a *homogeneous and isotropic* material. In this special case, the viscosity tensor assumes the form

$$\mathbb{V}_{IKV} = \zeta\, \hat{\mathbf{I}} \otimes \hat{\mathbf{I}} + 2\eta\, \mathbb{P} = (\zeta - \frac{2}{3}\eta)\, \hat{\mathbf{I}} \otimes \hat{\mathbf{I}} + 2\eta\, \mathbb{I}\,, \qquad (29)$$

depending on two material constants: *bulk viscosity* ζ and *shear viscosity* η.

To compute $\partial_t \hat{\mathbf{E}}'$ we use the expression (24) for the modified Green–Lagrange strain tensor of a Cosserat rod including the small strain approximation (19), with the result[15]

$$\partial_t \hat{\mathbf{E}}' \approx \frac{1}{2}\left[\partial_t \mathbf{H} \otimes \mathbf{a}_0^{(3)} + \mathbf{a}_0^{(3)} \otimes \partial_t \mathbf{H}\right] - \nu\, \partial_t H_3 \left[\hat{\mathbf{I}} - \mathbf{a}_0^{(3)} \otimes \mathbf{a}_0^{(3)}\right] \qquad (30)$$

---

[14]Note that $\hat{\mathbf{S}}_v : \partial_t \hat{\mathbf{E}} = 2\Psi_{KV}(\partial_t \hat{\mathbf{E}})$ corresponds to the *viscous stress power density*, such that the integral $P_v(t) := 2\int_V dV\, \Psi_{KV}(\partial_t \hat{\mathbf{E}})$ over the body volume yields the (time dependent) rate at which a Kelvin–Voigt solid dissipates mechanical energy under approximately isothermal conditions near thermodynamic equilibrium, (see Ch. V §34 & §35) of Landau and Lifshitz (1986)). For a thorough discussion of the role of the dissipation function within the theory of small fluctuations near thermodynamic equilibrium from the viewpoint of statistical physics we refer to the the corresponding paragraphs in ch. XII in Landau and Lifshitz (1980) (in particular §121), as well as V. Berdichevsky's recent article 2003. In section VI of the latter, the author points out that a Kelvin–Voigt type constitutive relation holds also at *finite* strains, with the dissipative part governed by a fourth order viscosity tensor $\mathbb{V}[\hat{\mathbf{E}}, \partial_t \hat{\mathbf{E}}]$ depending on the local strain and its rate. While a dependence of $\mathbb{V}$ on the invariants of $\partial_t \hat{\mathbf{E}}$ in general prevents the existence of a dissipation function, the latter *does* indeed exist according to V.B.'s arguments if $\mathbb{V} = \mathbb{V}[\hat{\mathbf{E}}]$ is independent of the strain rate. This holds e.g. in the case of the Kelvin–Voigt limit of constitutive laws belonging to the class of *finite linear viscoelasticity* (Coleman and Noll, 1961) at sufficiently small strain rates (i.e. sufficiently slow deformations of a body).

[15]Computing $\partial_t \hat{\mathbf{E}}'$ from (24) leads to the identity $\partial_t E_{\alpha\alpha} = -\nu\, \partial_t E_{33} \approx -\nu\, \partial_t H_3$ likewise obtained from (30). This implies that the relation $E_{\alpha\alpha} = -\nu E_{33}$ between in–plane to out–of–plane normal strains remains valid also for *dynamic* motions (at least for sufficiently slow ones), and that *Poisson's ratio* ν may still be treated as a *constant* in this case (see also Christensen, 1982, sec. 2.3).

depending on the time derivative $\partial_t \mathbf{H}(\xi_1, \xi_2, s, t) = \partial_t H_k(\xi_1, \xi_2, s, t) \, \mathbf{a}_0^{(k)}(s)$ of the material strain vector with components

$$
\begin{aligned}
\partial_t H_1(\xi_2, s, t) &= \partial_t V_1(s, t) - \xi_2 \, \partial_t U_3(s, t) \,, \\
\partial_t H_2(\xi_1, s, t) &= \partial_t V_2(s, t) + \xi_1 \, \partial_t U_3(s, t) \,, \\
\partial_t H_3(\xi_1, \xi_2, s, t) &= \partial_t V_3(s, t) + \xi_2 \, \partial_t U_1(s, t) - \xi_1 \, \partial_t U_2(s, t) \,,
\end{aligned} \tag{31}
$$

i.e.: $\hat{\mathbf{R}}_0^T \cdot \partial_t \mathbf{H} = (\partial_t H_k) \, \mathbf{e}_k = \partial_t \mathbf{V} - \xi_\alpha \mathbf{e}_\alpha \times \partial_t \mathbf{U}$, written as a cartesian vector w.r.t. the global basis $\{\mathbf{e}_1, \mathbf{e}_2, \mathbf{e}_3\}$.

Inserting (30) and (31) into the dissipation density function $\Psi_{IKV}(\partial_t \hat{\mathbf{E}}') = \frac{1}{2} \partial_t \hat{\mathbf{E}}' : \mathbb{V}_{IKV} : \partial_t \hat{\mathbf{E}}'$ of the isotropic Kelvin–Voigt model, analogous computational steps as those done for the derivation of the stored energy $\Psi_{SVK}(\hat{\mathbf{E}}')$ in the previous subsection yield the expression

$$
2\Psi_{IKV}(\partial_t \hat{\mathbf{E}}) \approx \eta_E \, (\partial_t H_3)^2 + \eta \left[(\partial_t H_1)^2 + (\partial_t H_2)^2 \right] \,,
$$

with the *extensional viscosity* parameter η_E as defined in (5) appearing as the prefactor[16] of $(\partial_t H_3)^2$. The computation of the cross section integrals of the squared time derivatives $(\partial_t H_k)^2$ yields the expressions

$$
\begin{aligned}
\left\langle (\partial_t H_3)^2 \right\rangle_{\mathcal{A}} &= A(\partial_t V_3)^2 + I_\alpha (\partial_t U_\alpha)^2 \,, \\
\left\langle (\partial_t H_1)^2 + (\partial_t H_2)^2 \right\rangle_{\mathcal{A}} &= A\left[(\partial_t V_1)^2 + (\partial_t V_2)^2 \right] + I_3 (\partial_t U_3)^2 \,,
\end{aligned}
$$

from which we obtain the desired cross section integral of the dissipation density function:

$$
\begin{aligned}
2 \left\langle \Psi_{IKV}(\partial_t \hat{\mathbf{E}}) \right\rangle_{\mathcal{A}} &\approx \eta_E A \, (\partial_t V_3)^2 + \eta_E I_\alpha \, (\partial_t U_\alpha)^2 \\
&\quad + \eta A \left[(\partial_t V_1)^2 + (\partial_t V_2)^2 \right] + \eta I_3 \, (\partial_t U_3)^2 \,.
\end{aligned} \tag{32}
$$

The dissipation function (11) of the Cosserat rod with diagonal damping coefficient matrices (3) and damping parameters (4) is then obtained as

$$
D_v \equiv D_{IKV} := \int_0^L ds \, \left\langle \Psi_{IKV}(\partial_t \hat{\mathbf{E}}') \right\rangle_{\mathcal{A}}
$$

by inserting the approximation of $\left\langle \Psi_{IKV}(\partial_t \hat{\mathbf{E}}') \right\rangle_{\mathcal{A}}$ given in (32).

---

[16]The term $K(1 - 2\nu)^2 + \frac{4}{3} G(1 + \nu)^2 = E$ analogously appears as the prefactor of H_3^2 in the expression (26) of the stored energy function of a Cosserat rod for the St.–Venant–Kirchhoff material.

4.1 Modification by shear correction factors

There is obviously a high degree of formal algebraic similarity in the derivations of the stored energy function (10) as presented in subsection 3.5 and the dissipation function (11) as presented above: Both functionals result by inserting the specific strain tensor (24) of a Cosserat rod or respectively its rate (30) into a volume integral over the 3D body domain of a density function defined as a quadratic form given by constant isotropic fourth order material tensors $\mathbb{H}$ and $\mathbb{V}$, making use of the same geometric as well as *"small strain"* approximations implied by the specific kinematical ansatz (15) for the configurations of a Cosserat rod. The formal analogy in the derivation procedure leads to a dissipation density (32) that may be obtained from its elastic counterpart (27) by substituting viscosity parameters for corresponding elastic moduli ($G \to \eta$, $E \to \eta_E$) and strain rates for strain measures.

In the case of the stored energy function (10) the effective stiffness parameters (2) of the rod model are obtained from a derivation using a kinematical ansatz that completely neglects out–of–plane warping (i.e.: $w_3 = 0 = \partial_k w_3$) due to transverse shearing and twisting, but accounts for in–plane warping (i.e.: $w_\alpha \neq 0$) in a simplified way by assuming a uniform lateral contraction (ULC) of the cross section according to the linear elastic theory (see section 3.4). Softening effects due to out–of–plane warping are then accounted for by introducing *shear correction factors* $0 < \varkappa_j \leq 1$, which in the case of a homogeneous and isotropic material enter the model as multipliers $A \to A_\alpha = A\varkappa_\alpha$ and $I_3 \to J_T = I_3\varkappa_3$ of the area A and polar moment I_3 of the cross section and — according to the linear theory — depend *solely* on the *cross section geometry*. The modified stiffness constants (7) are obtained in combination with the elastic moduli $G = \mu$ and E, the latter appearing instead of $\lambda + 2\mu$ due to the enforcment of vanishing in–plane stresses by allowing for ULC according to (24).

Although the derivation of explicit formulas[17] for $\varkappa_j$ is carried out for *static* boundary value problems, the same $\varkappa_j$, as well as the kinematic ansatz accounting for ULC, may be used for *dynamic* problems, due to the negligible influence of dynamic effects on the warping behaviour of cross sections, provided that the rod geometry is sufficiently slender. Therefore the geometric modifications $A \to A_\alpha = A\varkappa_\alpha$ and $I_3 \to J_T = I_3\varkappa_3$, which have already been used to provide modified stiffness parameters (7) for an improved approximation of the 3D (volumetric) *elastic energy* by the stored energy function (10) in the static as well as in the dynamic case, remain likewise valid to achieve a comparable improvement for the approximation of the 3D integrated *viscous stress power* by the dissipation function (11), with modified damping param-

---

[17]We refer to footnote 13 for a discussion of this issue.

24

eters given by (8), leading to the modified expressions (9) for the effective viscosity matrices.

This completes our derivation of the Kelvin–Voigt type dissipation function of a Cosserat rod. Although the arguments given above would certainly benefit from a mathematical confirmation by rigorous (asymptotic) analysis, the latter is beyond the scope of this work.

4.2 An (erroneous) alternative derivation approach

The formulation of the Cosserat rod model given by Simo (1985) introduces spatial force and moment vectors $\mathbf{f}$ and $\mathbf{m}$, usually denoted as *stress resultants* and *stress couples*, as the cross section integrals

$$
\begin{aligned}
\mathbf{f}(s,t) &= \left\langle \hat{\mathbf{P}}(\xi_1, \xi_2, s, t) \cdot \mathbf{a}_0^{(3)}(s) \right\rangle_{\mathcal{A}} , \\
\mathbf{m}(s,t) &= \left\langle \xi(s) \times \hat{\mathbf{P}}(\xi_1, \xi_2, s, t) \cdot \mathbf{a}_0^{(3)}(s) \right\rangle_{\mathcal{A}}
\end{aligned}
$$

of the traction forces of the 1st Piola–Kirchhoff stress tensor acting on the cross section area and the corresponding moments generated by the Piola–Kirchhoff tractions w.r.t. the cross section centroid, which are obtained by means of the "lever arm" vector $\xi(s) = \xi_\alpha \mathbf{a}_0^{(\alpha)}(s)$. Both integrants may be expressed in terms of the 2nd Piola–Kirchhoff stress by means of the transformation $\hat{\mathbf{P}} = \hat{\mathbf{F}} \cdot \hat{\mathbf{S}}$ with the deformation gradient. In view of the small strain approximation $\hat{\mathbf{P}} \approx \hat{\mathbf{R}}_{rel} \cdot \hat{\mathbf{S}}$ with $\hat{\mathbf{S}} \approx \mathbb{H} : \hat{\mathbf{E}}$ discussed in subsection 3.3 we obtain the relations

$$
\begin{aligned}
\hat{\mathbf{R}}_0(s) \cdot \mathbf{F}(s,t) &\approx \left\langle \hat{\mathbf{S}}(\xi_1, \xi_2, s, t) \cdot \mathbf{a}_0^{(3)}(s) \right\rangle_{\mathcal{A}} , \\
\hat{\mathbf{R}}_0(s) \cdot \mathbf{M}(s,t) &\approx \left\langle \xi(s) \times \hat{\mathbf{S}}(\xi_1, \xi_2, s, t) \cdot \mathbf{a}_0^{(3)}(s) \right\rangle_{\mathcal{A}}
\end{aligned}
$$

connecting the spatial stress resultants $\mathbf{f} = \hat{\mathbf{R}} \cdot \mathbf{F}$ and stress couples $\mathbf{m} = \hat{\mathbf{R}} \cdot \mathbf{M}$ to their material counterparts rotated to the local reference frame $\hat{\mathbf{R}}_0(s) = \mathbf{a}_0^k(s) \otimes \mathbf{e}_k$.

Expanding the material force and moment vectors w.r.t. the local ONB given by the reference frame $\hat{\mathbf{R}}_0(s)$ as $\hat{\mathbf{R}}_0(s) \cdot \mathbf{F}(s,t) = F_k(s,t)\, \mathbf{a}_0^k(s)$ and $\hat{\mathbf{R}}_0(s) \cdot \mathbf{M}(s,t) = M_k(s,t)\, \mathbf{a}_0^k(s)$ yields their components in terms of the cross section integrals

$$
F_j = \left\langle S_{j3} \right\rangle_{\mathcal{A}} \quad , \quad M_1 = \left\langle \xi_2 S_{33} \right\rangle_{\mathcal{A}} \, , \quad M_2 = \left\langle -\xi_1 S_{33} \right\rangle_{\mathcal{A}} \, ,
$$
$$
M_3 = \left\langle \xi_1 S_{23} - \xi_2 S_{13} \right\rangle_{\mathcal{A}}
$$

of the components of $\hat{\mathbf{S}}$ w.r.t. this basis. To compute these components of the material force and moment vectors in closed form for the special case

$\hat{\mathbf{S}}' = \mathbb{H}_{SVK} : \hat{\mathbf{E}}' + \mathbb{V}_{IKV} : \partial_t \hat{\mathbf{E}}' = \hat{\mathbf{S}}'_{SVK} + \hat{\mathbf{S}}'_{IKV}$ with the approximate expressions (24) and (30) of the Green–Lagrange strain tensor and its rate and the constant isotropic material tensors $\mathbb{H}_{SVK} = K\,\hat{\mathbf{I}} \otimes \hat{\mathbf{I}} + 2G\,\mathbb{P}$ and $\mathbb{V}_{IKV} = \zeta\,\hat{\mathbf{I}} \otimes \hat{\mathbf{I}} + 2\eta\,\mathbb{P}$, we have to evaluate the cross section integrals with the stress components $S'_{\alpha 3} = GH_\alpha + \eta \partial_t H_\alpha$ and $S'_{33} = EH_3 + \tilde{\eta}_E \partial_t H_3$, with $\tilde{\eta}_E := (1 - 2\nu)\zeta + (1 + \nu)\frac{4}{3}\eta$ multiplying the strain rate $\partial_t H_3 \approx \partial_t E_{33}$.

Therefore $\tilde{\eta}_E$ has to be interpreted as extensional viscosity, but obviously differs from the expression η_E given in (5) and derived above by computing the dissipation function. Therefore the corresponding retardation time constant $\tilde{\tau}_E := \tilde{\eta}_E/E = \frac{1}{3}(\tau_B + 2\tau_S)$, which is independent of the value of Poisson's ratio ν, likewise differs from the expression of the extensional retardation time τ_E given in (6). Both expressions $\tilde{\eta}_E$ and η_E yield extensional viscosity as a combination of shear and bulk viscosity, but agree only in the special case $\nu = 0$. The same assertion likewise holds for the corresponding retardation times, of course. However, only η_E yields the correct incompressible limit $\eta_E \to 3\eta$ for $\nu \to \frac{1}{2}$, while $\tilde{\eta}_E$ tends to the smaller (and incorrect) value of 2η in this case.

The resulting expressions for the material force components are given by

$$F_\alpha = GA\left[V_\alpha + \tau_S\,\partial_t V_\alpha\right] , \quad F_3 = EA\left[(V_3 - 1) + \tilde{\tau}_E\,\partial_t V_\alpha\right] ,$$

and the material moment components correspondingly by

$$\begin{aligned} M_\alpha &= EI_\alpha\left[(U_\alpha - U_{0\alpha}) + \tilde{\tau}_E\,\partial_t U_\alpha\right] , \\ M_3 &= GI_3\left[(U_3 - U_{03}) + \tau_S\,\partial_t U_3\right] . \end{aligned}$$

A comparison with the stiffness and damping parameters (2) and (6) entering the constitutive equations (1) shows that the derivation approach sketched above correctly yields *all* of the stiffness parameters as well as the damping parameters associated to transverse and torsional shear deformations. However, the damping parameters governed by normal stresses and extensional viscosity do not agree due to the appearance of $\tilde{\tau}_E$ instead of the correct time constant τ_E.

The discrepancy between the results of both derivation approaches can be traced back to the fact that the integration of the traction forces and their associated moments over the cross section fails to account for the non–vanishing contributions of the in–plane strain rates $\partial_t E'_{\alpha\alpha} = -\nu \partial_t H_3$ associated to uniform lateral contraction to the total energy dissipation of the rod. Paired with the corresponding viscous stress components $S'_{\alpha\alpha} = [(1-2\nu)\zeta - (1+\nu)\eta]\partial_t H_3$ these result in the (in general non–vanishing) contribution

$$\begin{aligned} S'_{\alpha\alpha}(\partial_t E'_{\alpha\alpha}) &= -2\nu\left[(1 - 2\nu)\zeta - (1 + \nu)\eta\right](\partial_t H_3)^2 \\ &= (\eta_E - \tilde{\eta}_E)(\partial_t H_3)^2 \end{aligned}$$

to the dissipation function. As the cross section integrals given above involve only the stress components $S'_{\alpha 3}$ and S'_{33}, this additional source of damping is, by definition, not contained in the resulting formulas for the material force and moment components F_j and M_j obtained via this approach.

However, this deficiency affects only the *viscous* part of the constitutive equations. The elastic part does not show any discrepancy, as the modified strain tensor (24) by construction provides vanishing in–plane elastic stress components (see section 3.4), such that the stored energy function does not contain any contributions from non–vanishing in–plane elastic stresses to the elastic energy, and the cross section integrals of the traction forces and their moments yield *all* stiffness parameters correctly.

In summary, the considerations above suggest that, also in the case of more general viscoelastic constitutive laws, our approach to derive effective constitutive equations for Cosserat rods by computing the stored energy and dissipation functions is superior to the alternative approach based on a direct computation of the forces and moments as resultant cross section integrals of the traction forces and associated moments, as the latter yields an effective extensional viscosity which is systematically too small for partially compressible and incompressible solids (i.e.: $0 < \nu \leq \frac{1}{2}$).

4.3 ANCF beams with Kelvin–Voigt damping

In the recent article of Abdel–Nasser and Shabana (2011), a damping model for geometrically nonlinear beams given in the ANCF (absolute nodal coordinates) formulation has been proposed. The authors obtained their model by inserting the 3D isotropic Kelvin–Voigt model as described above into their ANCF element ansatz. They used the Lamé parameters λ and μ as elastic moduli, and introduced corresponding viscosity parameters λ_v and μ_v, which they related to the elastic moduli by *dissipation factors* γ_{v1} and γ_{v2}. From the context it seems clear that in our notation $\gamma_{v2} = \tau_S$, such that $\mu_v = G\tau_S = \eta$. Likewise we may identify $\gamma_{v1} = \tau_B$, such that $\lambda_v = K\tau_B - \frac{2}{3}G\tau_S = \zeta - \frac{2}{3}\eta$, and the viscosities are related by the same relation as the elastic moduli (i.e.: $\lambda = K - \frac{2}{3}G$). If the ANCF ansatz chosen in (Abdel–Nasser and Shabana, 2011) handles lateral contraction effects correctly, both models should behave similar and yield similar simulation results. However, the appearance of the unmodified elastic moduli $\lambda = 2\mu\nu/(1-2\nu)$ and $\lambda + 2\mu = 2\mu(1-\nu)/(1-2\nu)$ in the element stiffness matrix (see eqn. (25) of the paper) indicates that the formulation chosen in (Abdel–Nasser and Shabana, 2011) may have problems in the case of incompressible materials ($\nu \to \frac{1}{2}$). A clarifying investigation of this issue as well as a detailed comparison of both models remains to be done in future work.

4.4   Validity of the Kelvin–Voigt model

As remarked already in Landau and Lifshitz (1986), the modelling of viscous dissipation for solids by a dissipation function of Kelvin–Voigt type is valid only for relatively slow processes near thermodynamic equilibrium, which means that the temperature within the solid should be approximately constant, and the macroscopic velocities of the material particles of the solid should be sufficiently slow w.r.t. the time scale of all internal relaxation processes.

To illustrate and quantify this statement, we briefly discuss the one–dimensional example of a linear viscoelastic stress–strain relation $\sigma(t) = \int_0^\infty d\tau\, G(\tau)\dot{\varepsilon}(t - \tau)$ governed by the relaxation function of a *generalized Maxwell model* given by $G(\tau) = G_\infty + \sum_{j=1}^N G_j \exp(-\tau/\tau_j)$, i.e. a *Prony series* (see e.g. Haupt, 2002). By Fourier transformation we obtain the relation $\hat{\sigma}(\omega) = \hat{G}(\omega)\hat{\varepsilon}(\omega)$ in the frequency domain, where the real and imaginary parts of the complex modulus function $\hat{G}(\omega) = G_\infty + \sum_{j=1}^N G_j \frac{i\tau_j\omega}{1+i\tau_j\omega}$ model the frequency dependent stiffness and damping properties of the material.

Using a 1D Kelvin–Voigt model $\sigma_{KV}(t) = G\varepsilon(t) + \eta\dot{\varepsilon}(t)$ we obtain the simple expression $\hat{\sigma}_{KV}(\omega) = [G + i\eta\omega]\hat{\varepsilon}(\omega)$, which approximates the generalized Maxwell model at sufficiently low frequencies with $G = G_\infty$ and $\eta = \sum_{j=1}^N G_j\tau_j$. The deviation between the generalized Maxwell model and its Kelvin–Voigt approximation may be estimated as

$$|\sigma(t) - \sigma_{KV}(t)| \;\leq\; \frac{1}{\pi}\sum_{j=1}^N G_j \int_0^\infty d\omega\, \frac{|\hat{\varepsilon}(\omega)|\,(\tau_j\omega)^2}{\sqrt{1 + (\tau_j\omega)^2}}\;.$$

This deviation may indeed become small, provided that the modulus $|\hat{\varepsilon}(\omega)|$ of the strain spectrum, which appears as a weighting factor for the terms of the sum on the r.h.s., takes on non–vanishing values only at frequencies much smaller than those given by the discrete spectrum of the inverse relaxation times $\omega_j = 1/\tau_j$. The estimate given above also shows that in this case the Kelvin–Voigt model provides a *low frequency approximation* of second order accuracy.
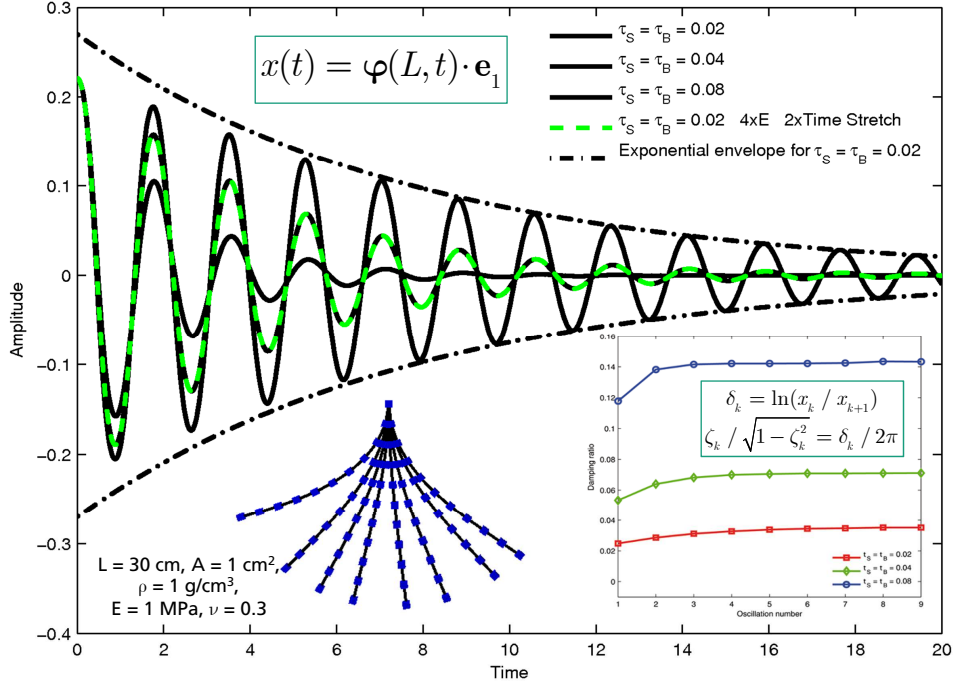
Figure 5: Damped non-linear bending vibrations of a clamped cantilever beam (see text for further details).

5 Numerical Examples

To illustrate the behaviour of our damping model, we show the results of numerical simulations of nonlinear vibrations of a cantilever beam in Fig. 5 obtained with the discrete Cosserat rod model presented in Lang et al. (2011).

The parameters of the beam are: length $L = 30\,\text{cm}$, quadratic cross-section area $A = 1 \times 1\,\text{cm}^2$, mass density $\rho = 1\,\text{g/cm}^3$, Young's modulus $E = 1\,\text{MPa}$, and Poisson's ratio $\nu = 0.3$. We assume that $\zeta/\eta = K/G$ holds for the viscosity parameters, such that according to our model (6) the values of all retardation time constants are equal ($\tau_B = \tau_S = \tau_E$). The tests were performed with three different values ($0.02\,\text{s}$, $0.04\,\text{s}$, and $0.08\,\text{s}$) of $\tau_E = \tau_{B/S}$. No gravitation is present.

The beam is fully clamped at one end, the other end is initially pulled sideways by applying a force $\mathbf{f}_L = F\mathbf{e}_1$ of magnitude $F = 0.05\,\text{N}$ to the other end. The resulting initial deformation state in static equilibrium[18] deviates

---

[18]A highly accurate approximation of this equilibrium configuration may be obtained as

far from the linear range of deformations governed by (infinitesimally) small displacements and rotations w.r.t. the reference configuration, while local strains are small in accordance with the constitutive assumptions. Starting from this initial equilibrium configuration, the beam is then released to vibrate transversally. The deformations of the beam shown in the inset of Fig. 5 are snapshots taken during the first half period of the oscillations which illustrate that in the initial phase of the oscillations substantial geometric nonlinearities are present. During the vibrations the beam remains in the plane of its initial deformation, such that all deformations are of plane bending type, and the extensional viscosity $\eta_E = E\tau_E$ becomes the main influence for damping.

As expected, the plots of the transverse oscillation amplitude $x(t) = \mathbf{e}_1 \cdot \boldsymbol{\varphi}(L, t)$ recorded at the free end of the beam show an exponential dying out in the range of small amplitudes (linear regime). The deviations from the exponential envelope adapted to the linear regime that are observed during the initial phase clearly show the influence of geometric nonlinearity. The plots also suggest that damping becomes weaker in the nonlinear range. However, linear behaviour seems to start already with the fifth oscillation period, where the amplitude still has a large value of $\approx L/3$.

This may be further analyzed by evaluating the *logarithmic decrements* $\delta_k = \ln(x(t_k)/x(t_{k+1}))$ recorded between succesive maxima $x(t_k)$ of the amplitude as well as the corresponding *damping ratios* ζ_k implicitely defined (see Craig and Kurdila, 2006, ch. 3.5, p. 75) by $\delta_k = 2\pi\zeta_k/\sqrt{1 - \zeta_k^2}$. The plots for the values of ζ_k determined in this way are shown in the inset of Fig. 5. As expected, the ratios approach constant values in the linear regime, which scale as $1 : 2 : 4$ proportional to the values of the time constant τ_E used in the simulations. The simulations also show that the decrements become lower in the range of large amplitudes, which confirms the observation that the damping effect of our Kelvin–Voigt model is extenuated by the presence of geometrical nonlinearity. Nevertheless, ζ_k still scales approximately proportional to τ_E also in the nonlinear range.

To investigate the influence of a variation of the bending stiffness on the damping behaviour, an additional test with quadrupled Young's modulus $E = 4\,\text{MPa}$ was performed. In the corresponding amplitude plot shown in Fig. 5 the time axis of the plot with quadrupled E was streched twofold, such that the oscillations could be compared directly. After time stretching the $(E = 4\,\text{MPa}, \tau_E = 0.02\,\text{s})$ plot coincides with the $(E = 1\,\text{MPa}, \tau_E = 0.04\,\text{s})$

---

the curve $s \mapsto \boldsymbol{\varphi}_{el}(s)$ and adapted frame $\hat{\mathbf{R}}_{el} = (\mathbf{e}_2 \times \partial_s \boldsymbol{\varphi}_{el}) \otimes \mathbf{e}_1 + \mathbf{e}_2 \otimes \mathbf{e}_2 + \partial_s \boldsymbol{\varphi}_{el} \otimes \mathbf{e}_3$ of an *inextensible Euler elastica*, which may be computed analytically in closed form in terms of Jacobian elliptic functions and elliptic integrals (see Love, 1927, ch. XIX §260–263) or (Landau and Lifshitz, 1986, ch. II §19).

plot, surprisingly even throughout the whole nonlinear range. Since the oscillation period T of the four times stiffer ($E = 4\,\mathrm{MPa}$) beam is twice smaller than that of the softer ($E = 1\,\mathrm{MPa}$) beam, this suggests that the damping ratio varies proportional to the ratio τ_E/T. Again this would be the expected behaviour in the linear regime, but is observed here in the nonlinear range as well.

For small amplitudes, the oscillation period may be estimated as $T \approx (2\pi/3.561)\,L^2\sqrt{\rho A/EI}$ using the well known formula for the fundamental transverse vibration frequency of a cantilever beam obtained from *Euler–Bernoulli* theory (see Craig and Kurdila, 2006, ch. 13.2, Ex. 13.3, eq. (8)). Inserting the parameters assumed above, we get $T \approx 1.81\,\mathrm{s}$ as an estimate, which correponds well to the time intervals of approximately $1.8\,\mathrm{s}$ between successive maxima shown in Fig. 5 that are also observed throughout the range of geometrically nonlinear deformations. For linear vibrations, damping ratio values $\zeta \approx 1$ correspond to a *critical* damping of the vibrating system, while values $0 < \zeta \ll 1$ indicate a *weak* damping. According to that, the values ζ_k observed in our experiments are in the range of weak to moderate damping, and are well approximated by the empirical formula $\zeta \approx \frac{1}{\pi}\tau_E/T$, such that critical damping of transverse vibrations would be observed at a value of $\tau_E \approx \pi T$. This provides a rough guideline for estimating the strenght of damping, or likewise an adjustment of the retardation time τ_E relative to the fundamental period T, if the Kelvin–Voigt model is utilized to provide artificial viscous damping in the sense of Antman (2003).

Corresponding experiments for axial or torsional vibrations are limited to the range of small vibrations amplitudes, similar to the ones shown by Abdel–Nasser and Shabana (2011), as for large amplitudes one would inevitably induce buckling to bending deformations, such that all deformation modes would occur simultaneously, which greatly hampers a systematic investigation of different damping effects in the geometrically nonlinear range. Nevertheless, experiments at small amplitudes are helpful to determine the ranges of weak, moderate and critical damping for the respective deformation modes, quantifyable by explicit formulas similar to the one given above for the case of transverse vibrations. These could then be used e.g. to adjust damping of different deformation modes to experimental obervations.

We also made a basic validation test for our discrete rod by comparing simulation results against those computed with Abaqus for a full volumetric model (3D) of the rod geometry. Although Abaqus does not readily provide a Kelvin–Voigt model, one may emulate it by adapting the parameters of a standard linear solid (SLS) material such that the latter approximates a Kelvin–Voigt solid. Fig. 6 shows that our model accurately reproduces the Abaqus 3D results.
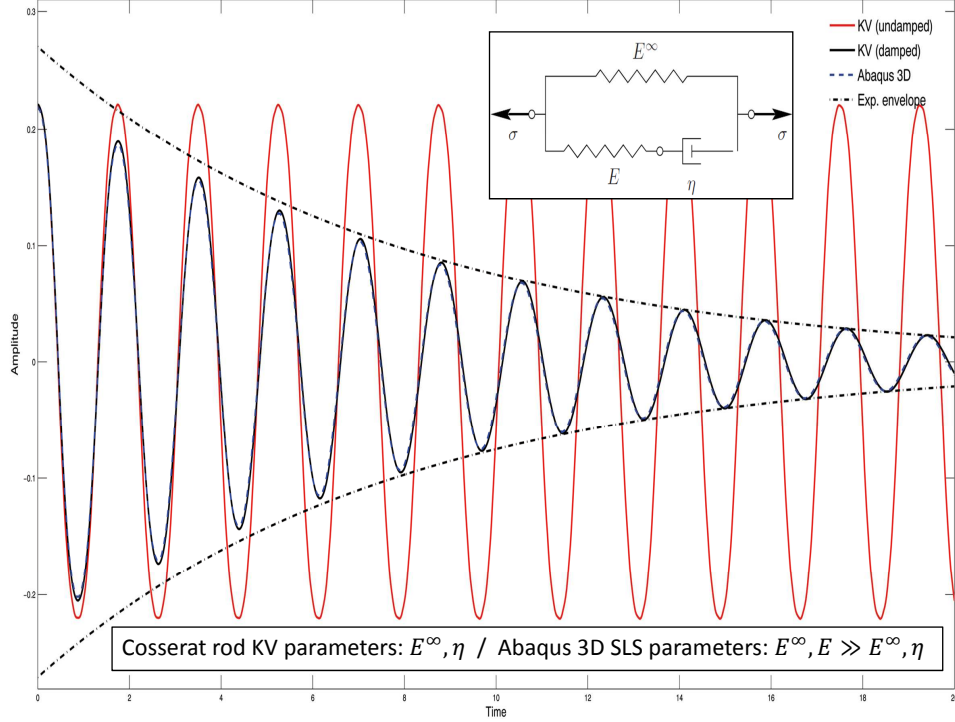
Figure 6: Damped non-linear bending vibrations of a clamped cantilever beam: Benchmark test simulations against Abaqus (3D) with a standard linear solid (SLS) material (plotted as dashed lines, approximately coinciding with the solid ones obtained with our model).

6 Conclusions

In our paper we presented the derivation of a viscous Kelvin–Voigt type damping model for geometrically exact Cosserat rods. For homogeneous and isotropic materials, we obtained explicit formulas for the damping parameters given in terms of the stiffness parameters and retardation time constants, assuming moderate reference curvatures, small strains and sufficiently low strain rates. In numerical simulations of transverse vibrations of a clamped cantilever beam we observed a weakening influence of geometric nonlinearities on the damping of the oscillation amplitudes. We also found that the variation of retardation time and bending stiffness has a similar effect on the damping ratio as in the linear regime.

References

Abdel–Nasser, A.M. and Shabana, A.A.: A nonlinear visco–elastic constitutive model for large rotation finite element formulations. Multibody System Dynamics, Vol. 26, No. 3, pp. 57–79, 2011.

Antman, S.S.: Invariant dissipative mechanisms for the spatial motion of rods suggested by artificial viscosity. Journal of Elasticity, Vol. 70, pp. 55–64, 2003.

Antman, S.S.: Nonlinear Problems of Elasticity (2nd Edition). Springer, 2005.

Arne, W., Marheineke, N., Schnebele, J. and Wegener, R.: Fluid–fiber–interaction in Rotational Spinning Process of Glass Wool Production. Journal of Mathematics in Industry, 1:2, doi:10.1186/2190-5983-1-2, 2011. Preprint: Reports of the ITWM, Nr. **197**, 2010.

Bauchau, O.A., Epple, A. and Heo, S.: Interpolation of Finite Rotations in Flexible Multibody Dynamics Simulations. Proc. of the Institution of Mechanical Engineers, Part K: Journal of Multi-body Dynamics, Vol. 222, Issue 3, pp. 353–366, 2008.

Bauchau, O.A.: Flexible Multibody Dynamics. Springer, 2011.

Berdichevsky, V.L.: On the energy of an elastic rod. J. Appl. Math. Mech. (PMM), Vol. 45, No. 4, pp. 518–529, 1981.

Berdichevsky, V.L., Staroselsky, L.A.: On the theory of curvilinear Timoshenko-type rods. J. Appl. Math. Mech. (PMM), Vol. 47, No. 6, pp. 809–816, 1983.

Berdichevsky, V.L.: Structure of equations of macrophysics. Phys. Rev. E, Vol. 68, Issue 6, 066126 pp. 1–26, 2003.

Berdichevsky, V.L.: Variational Principles of Continuum Mechanics, Vol. I: Fundamentals, Vol. II: Applications. Springer, 2009.

Bergou, M., Wardetzky, M., Robinson, S., Audoly, B. and Grinspun, E.: Discrete Elastic Rods. ACM Transaction on Graphics (SIGGRAPH), Vol. 27, No. 3, pp. 63:1–63:12, 2008.

Bergou, M., Audoly, B., Vouga, E., Wardetzky, M. and Grinspun, E.: Discrete Viscous Threads. ACM Transaction on Graphics (SIGGRAPH), Vol. 29, Nr. 4, pp. 116:1–116:10, 2010.

Chao, I., Pinkall, U., Sanan, P. and Schröder, P.: A Simple Geometric Model for Elastic Deformations. ACM Transaction on Graphics (SIGGRAPH), Vol. 29, Nr. 4, pp. 38:1–38:6, 2010.

Coleman, B.D. and Noll, W.: Foundations of Linear Viscoelasticity. Rev. Mod. Phys., Vol. 33, No. 2, pp. 239–249, 1961.

Cowper, G.R.: The shear coefficient in Timoshenko's beam theory. J. Appl. Mech., Vol. 33, pp. 335–340, 1966.

Craig, R.R. and Kurdila, A.J.: Fundamentals of Structural Dynamics (2nd Edition). John Wiley & Sons, 2006.

Christensen, R.M.: Theory of Viscoelsaticity (2nd Edition). Academic Press, 1982.

Dong, S.B., Alpdogan, C., and Taciroglu, E.: Much ado about shear correction factors in Timoshenko beam theory. Int. J. Solids Struct., Vol. 47, Issue 13, pp. 1651–1665, 2010.

Géradin, M. and Cardona, A.: Flexible Multibody Dynamics: A Finite Element Approach. John Wiley & Sons, 2001.

Gruttmann, F. and Wagner, W.: Shear correction factors in Timoshenko's beam theory for arbitrary shaped cross sections. Computational Mechanics, Vol. 27, pp. 199–207, 2001.

Gurtin, M.E.: The Linear Theory of Elasticity, in S. Flügge, C. Truesdell (eds.): Handbuch der Physik Vol. VIa/2 – Mechanics of Solids II, pp. 1–295, Springer, Berlin, 1972.

Gurtin, M.E.: An Introduction to Continuum Mechanics, Academic Press, 1981.

Haupt, P.: Continuum Mechanics an the Theory of Materials (2nd edition), Springer, 2002.

Hodges, D.H.: Nonlinear Composite Beam Theory. AIAA, 2006.

Irschik, H. and Gerstmayr, J.: A continuum mechanics based derivation of Reissner's large-displacement finite-strain beam theory: The case of plane deformations of originally straight Bernoulli–Euler beams. Acta Mechanica, Vol. 206, pp. 1–21, 2009.

Humer, A. and Irschik, H.: Large deformation and stability of an extensible elastica with an unknown length. Int. J. Solids Struct., Vol. 48, pp. 1301–1310, 2011.

Jung, P., Leyendecker, S., Linn, J., and Ortiz, M.: A discrete mechanics approach to the Cosserat rod theory – Part 1: static equilibria. Int. J. Numer. Methods Eng., Vol. 85, No. 1, pp. 31–60, 2011. Preprint: Reports of the ITWM, Nr. **183**, 2010.

Kapania, R.K. and Li, J.: On a geometrically exact curved/twisted beam theory under rigid cross–section assumption. Computational Mechanics, Vol. 30, pp. 428–443, 2003.

Klar, A., Marheineke, N. and Wegener, R.: Hierarchy of Mathematical Models for Production Processes of Technical Textiles. ZAMM, Vol. 89(12), pp. 941–961, 2009. Preprint: Reports of the ITWM, Nr. **156**, 2009.

Landau, L.D. and Lifshitz, E.M.: Statistical Physics – Part 1 (Course of Theoretical Physics Vol. 5, 3rd ed.). Butterworth Heinemann, 1980.

Landau, L.D.; Lifshitz, E.M.: Theory of Elasticity (Course of Theoretical Physics Vol. 7, 3rd ed.). Butterworth Heinemann, 1986.

Lang, H., Linn, J., and Arnold, M.: Multibody dynamics simulation of geometrically exact Cosserat Rods. Multibody System Dynamics, Vol. 25, No. 3, pp. 285–312, 2011. Preprint: Reports of the ITWM, Nr. **209**, 2011.

Lang, H. and Arnold, M.: Numerical aspects in the dynamic simulation of geometrically exact rods. Applied Numerical Mathematics, Vol. 62, pp. 1411–1427, 2012. Preprint: Reports of the ITWM, Nr. **179**, 2009.

Lemaitre, J. and Chaboche, J.-L.: Mechanics of Solid Materials. Cambridge Universtity Press, 1990.

Lemaitre, J., Chaboche, J.-L., Benallal, A., Desmorat, R.: Mécanique des Matériaux Solides (3e Édition). Dunod, Paris, 2009.

Linn, J., Stephan, T., Carlsson, J. and Bohlin, R.: Fast Simulation of Quasistatic Rod Deformations for VR Applications. L.L. Bonilla, M. Moscoso, G. Platero and J.M. Vega (Eds.): *Progress in Industrial Mathematics at ECMI 2006*, pp. 247–253, ISBN 978-3-540-71992-2, Springer, 2008. Preprint: Reports of the ITWM, Nr. **143**, 2008.

Linn, J., Lang, H., and Tuganov, A.: Geometrically exact Cosserat rods with Kelvin–Voigt type viscous damping. Proceedings of the 2nd Joint International Conference on Multibody System Dynamics (IMSD2012), Stuttgart, Germany, P. Eberhard and P. Ziegler (Eds.), ISBN 978-3-927618-32-9, 2012. Preprint: Reports of the ITWM, Nr. **218**, 2012.

Linn, J., Lang, H., and Tuganov, A.: Geometrically exact Cosserat rods with Kelvin–Voigt type viscous damping. Mechanical Sciences, Vol. 4, pp. 79–96, 2013. Available for download at www.mech-sci.net/4/79/2013/

Lorenz, M., Marheineke, N., and Wegener, R.: On an asymptotic upper–convected Maxwell model for a viscoelastic jet. Proc. Appl. Math. Mech. (PAMM), Vol. 12, No. 1, pp. 601–602, 2012.

Love, A.E.H.: A Treatise on the Mathematical Theory of Elasticity. 4th edition (1927), reprinted by Dover, New York, 1963.

Mata, P., Oller, S. and Barbat, A.H.: Static analysis of beam structures under nonlinear geometric and constitutive behavior. Comput. Meth. Appl. Mech. Eng., Vol. 196, No. 45-48 pp. 4458–4478, 2007.

Mata, P., Oller, S. and Barbat, A.H.: Dynamic analysis of beam structures considering geometric and constitutive nonlinearity. Comput. Meth. Appl. Mech. Eng., Vol. 197, No. 6-8 pp. 857–878, 2008.

Marheineke, N. and Wegener, R.: Asymptotic Model for the Dynamics of Curved Viscous Fibers with Surface Tension. J. Fluid Mech., Vol. 622, pp. 345–369, 2009. Preprint: Reports of the ITWM, Nr. **115**, 2007.

Panda, S., Marheineke, N. and Wegener, R.: Systematic Derivation of an Asymptotic Model for the Dynamics of Curved Viscous Fibers. Math. Meth. Appl. Sci., Vol. 31, pp. 1153–1173, 2008. Preprint: Reports of the ITWM, Nr. **86**, 2006.

Petrie, C.J.S: Extensional viscosity: A critical discussion. J. Non–Newtonian Fluid Mech., Vol. 137, pp. 15–23, 2006.

Ribe, N.M.: Coiling of viscous jets. Proc. R. Soc. Lond. A, Vol. 460, No. 2051, pp. 3223–3239, 2004.

Romero, I.: A comparison of finite elements for nonlinear beams: the absolute nodal coordinate and geometrically exact formulations. Multibody System Dynamics, Vol. 20, pp. 51–68, 2008.

Schulze, M., Dietz, S., Tuganov, A., Lang, H., and Linn, J.: Integration of nonlinear models of flexible body deformation in Multibody System Dynamics. Proceedings of the 2nd Joint International Conference on Multibody System Dynamics (IMSD2012), Stuttgart, Germany, P. Eberhard and P. Ziegler (Eds.), ISBN 978-3-927618-32-9, 2012. Preprint: Reports of the ITWM, Nr. **219**, 2012.

Simo, J.C., Hjelmstad, K.D. and Taylor, R.L.: Numerical formulations of elasto-viscoplastic response of beams accounting for the effect of shear. Comput. Meth. Appl. Mech. Eng., Vol. 42, No. 3, pp. 301–330, 1984.

Simo, J.C.: A finite strain beam formulation: the three dimensional dynamic problem – Part I. Comput. Meth. Appl. Mech. Eng., Vol. 49, No. 1, pp. 55–70, 1985.

Trouton, F.T.: On the coefficient of viscous traction and its relation to that of viscosity. Proc. R. S. Lond. A, Vol. 77, pp. 426–440, 1906.

Villagio, P.: Mathematical Models for Elastic Structures, Cambridge University Press, 1997 (digital paperback reprint: 2005).

Weiss, H.: Dynamics of Geometrically Nonlinear Rods: I — Mechanical Models and Equations of Motion. Nonlinear Dynamics, Vol. 30, pp. 357–381, 2002.

Weiss, H.: Dynamics of Geometrically Nonlinear Rods: II — Numerical Methods and Computational Examples. Nonlinear Dynamics, Vol. 30, pp. 383–415, 2002.

Zupan, E., Saje, M. and Zupan, D.: The quaternion-based three-dimensional beam theory. Comput. Meth. Appl. Mech. Eng., Vol. 198, pp. 3944–3956, 2009.

Zupan, E., Saje, M. and Zupan, D.: Quaternion-based dynamics of geometrically nonlinear spatial beams using the Runge–Kutta method. Finite Elements in Analysis and Design, Vol. 54, pp. 48–60, 2012.

Zupan, E., Saje, M. and Zupan, D.: Dynamics of spatial beams in quaternion description based on the Newmark integration scheme. Computational Mechanics, Vol. 51, No. 1, pp. 47–64, 2012.

A   Measuring 3D strains and stresses for rods

From a mathematical point of view, the tensor $\hat{\mathbf{C}}$ may be regarded as the fundamental quantity to decribe the *shape* of a body, as it corresponds to the *metric* which determines the shape up to rigid body motions, provided that certain integrability conditions (i.e.: the vanishing of the Riemann curvature tensor) are satisfied. Other strain measures may be obtained as invertible functions of $\hat{\mathbf{C}}$ via its *spectral decomposition*. As a supplement to the brief discussion given in section 3.1, we mention a few alternatives to measure 3D strains and stresses used elsewhere in connection with geometrically exact rod theory.

A.1   The Biot strain and its approximation

In the case of small strains, the *Biot* strain tensor defined as $\hat{\mathbf{E}}_B := \hat{\mathbf{U}} - \hat{\mathbf{I}}$, with the *right stretch tensor* $\hat{\mathbf{U}}$ given *implicitely* either by the polar decompostion $\hat{\mathbf{F}} = \hat{\mathbf{R}}_{pd} \cdot \hat{\mathbf{U}}$ of the deformation gradient, or as $\hat{\mathbf{U}} = \hat{\mathbf{C}}^{1/2}$ in terms of the right Cauchy–Green tensor, is likewise an appropriate alternative choice of a frame–indifferent material strain measure. Due to the algebraic identity $\hat{\mathbf{E}} = \frac{1}{2}(\hat{\mathbf{U}}^2 - \hat{\mathbf{I}}) = \frac{1}{2}(\hat{\mathbf{I}} + \hat{\mathbf{U}}) \cdot \hat{\mathbf{E}}_B$ the Biot and Green–Lagrange strains agree up to leading order for small strains, i.e.: $\hat{\mathbf{E}} \approx \hat{\mathbf{E}}_B$ holds whenever $\hat{\mathbf{U}} \approx \hat{\mathbf{I}}$.

One might argue that for small strains it is preferable to use $\hat{\mathbf{E}}_B$ as a strain measure, as it is *linear* in $\hat{\mathbf{U}}$ and therefore a first order quantity in terms of in the principal stretches, different from $\hat{\mathbf{E}}$, which is quadratic in $\hat{\mathbf{U}}$. However, while (18) provides a *kinematically exact* expression for $\hat{\mathbf{I}} + 2\hat{\mathbf{E}} = \hat{\mathbf{C}} = \hat{\mathbf{U}}^2$, a comparably simple closed form expression for $\hat{\mathbf{U}}$ itself is not available. In general the tensor $\hat{\mathbf{U}}$ has to be constructed via the spectral decomposition of $\hat{\mathbf{C}}$ (see below), which in 3D cannot be expressed easily[19] in closed form.

Only for special simplified problems, like the *plane* deformation of an extensible Kirchhoff rod as discussed by Irschik and Gerstmayr (2009) and Humer and Irschik (2011), it is possible to derive simple, kinematically exact closed form expressions for $\hat{\mathbf{U}}$ and $\hat{\mathbf{R}}_{pd}$ by inspection of the deformation gradient: In this special case, or likewise in the more general case of twist–free spatial deformations of Kirchhoff rods (i.e.: extensible *Elastica*), $\mathbf{H} = H_3 \, \mathbf{a}_0^{(3)}$ holds due to $H_\alpha \equiv 0$, such that the exact expressions $\hat{\mathbf{R}}_{pd} = \hat{\mathbf{R}}_{rel}$ and $\hat{\mathbf{U}} = \hat{\mathbf{I}} + (H_3/J_0) \, \mathbf{a}_0^{(3)} \otimes \mathbf{a}_0^{(3)}$ may be read off directly from (16) due to the uniqueness of the polar decomposition.

---

[19]Whereas analytical expressions for the *eigenvalues* of a 3D symmetric matrix are provided by Cardano's formulas, we are not aware of any simple closed form expression for the *eigenvectors*.

Spectral decomposition of the right Cauchy–Green tensor

The *spectral decomposition* $\hat{\mathbf{C}} = \sum_{k=1}^{3} \lambda_k^2 \, \mathbf{N}_k \otimes \mathbf{N}_k$ of the right CG tensor (Gurtin, 1972, 1981, see) is given in terms of the eigenvalues $\lambda_k^2 \geq 0$ and the corresponding triple $\{\mathbf{N}\}_{k=1,2,3}$ of orthonormal eigenvectors solving the eigenvalue problem $\hat{\mathbf{C}} \cdot \mathbf{N}_k = \lambda_k^2 \, \mathbf{N}_k$ with $\mathbf{N}_k \cdot \mathbf{N}_l = \delta_{kl}$. The spectral decomposition of $\hat{\mathbf{E}}_B$ is constructed from the same eigenvectors and the principle stretches $\lambda_k = \sqrt{\lambda_k^2}$ as $\hat{\mathbf{E}}_B = \sum_{k=1}^{3}(\lambda_k - 1) \, \mathbf{N}_k \otimes \mathbf{N}_k$.

In the special case discussed above, the spectral problems for $\hat{\mathbf{C}}$ and $\hat{\mathbf{U}} = \hat{\mathbf{C}}^{1/2}$ become trivial: One eigenvector of $\hat{\mathbf{U}}$ is given by $\mathbf{a}_0^{(3)}$ with eigenvalue $(1 + H_3/J_0)$, any vector located in the cross section plane orthogonal to $\mathbf{a}_0^{(3)}$ is also an eigenvector with eigenvalue 1, and the eigenvectors of $\hat{\mathbf{C}}$ are the same, with squared eigenvalues $(1 + H_3/J_0)^2$ and 1.

Also in the more general case of $\hat{\mathbf{C}}$ given by (18) with a non-zero projection $\mathbf{H}_\perp := \mathbf{a}_0^{(3)} \times (\mathbf{H} \times \mathbf{a}_0^{(3)}) = H_\alpha \, \mathbf{a}_0^{(\alpha)}$ of $\mathbf{H}$ onto the cross section with norm $H_\perp := \|\mathbf{H}_\perp\| = (H_1^2 + H_2^2)^{1/2}$ an analytical solution of the spectral problem is possible: By inspection $\mathbf{N}_3 := \mathbf{H} \times \mathbf{a}_0^{(3)}/H_\perp$ is found as one of the eigenvectors with eigenvalue $\lambda_3^2 = 1$. The eigenvectors

$$\mathbf{N}_1 = \cos(\phi)\,\mathbf{h}_\perp + \sin(\phi)\,\mathbf{a}_0^{(3)} \, , \quad \mathbf{N}_2 = -\sin(\phi)\,\mathbf{h}_\perp + \cos(\phi)\,\mathbf{a}_0^{(3)}$$

are located in the plane orthogonal to $\mathbf{N}_3$ spanned by the two orthogonal vectors $\mathbf{h}_\perp := \mathbf{H}_\perp/H_\perp$ and $\mathbf{a}_0^{(3)}$. The remaining 2D spectral problem in this plane may then be solved analytically by a *Jacobi rotation* that diagonalizes the matrix representing $\hat{\mathbf{C}}$ w.r.t. the rotated basis $\{\mathbf{N}_1, \mathbf{N}_2\}$. The roots of the characteristic polynomial yield the pair

$$\lambda_\pm^2 = 1 + E_{33} \pm \sqrt{E_{33}^2 + (H_\perp/J_0)^2}$$

of eigenvalues with $E_{33} = H_3/J_0 + \frac{1}{2}(\mathbf{H}/J_0)^2$ (see (20)).

The condition $\mathbf{N}_1^T \cdot \hat{\mathbf{C}} \cdot \mathbf{N}_2 \equiv 0$ provides the equation

$$(H_\perp/J_0)\cos(2\phi) + E_{33}\sin(2\phi) = 0$$

that implicitely determines the angle ϕ. The spectral problem for the modified tensor $\hat{\mathbf{C}}' = \hat{\mathbf{I}} + 2\hat{\mathbf{E}}'$ given by (24) is solvable by the same procedure: $\mathbf{N}_3 = \mathbf{H} \times \mathbf{a}_0^{(3)}/H_\perp$ remains an eigenvector with shifted eigenvalue $\lambda_3'^2 = 1 - 2\nu E_{33}$, the likewise shifted eigenvalues $\lambda_\pm'^2$ of $\hat{\mathbf{C}}'$ are given by

$$\lambda_\pm'^2 = 1 + (1-\nu)E_{33} \pm \sqrt{((1+\nu)E_{33})^2 + (H_\perp/J_0)^2} \, ,$$

and the angle ϕ' is implicitely determined by

$$(H_\perp/J_0)\cos(2\phi') + (1+\nu)E_{33}\sin(2\phi') = 0 \, .$$

Approximation for small strains

These considerations show that, although a kinematically exact closed form expressions of $\hat{\mathbf{E}}_B$ or $\hat{\mathbf{E}}'_B$ for deformed configurations of a Cosserat rod ($\mathbf{H} \neq \mathbf{0}$) may be obtained, these consists of algebraically rather complicated expressions in terms of the components of vector $\mathbf{H}/J_0$, compared to the relatively simple formula (18) for the Green–Lagrange strain. Otherwise, we may consider $\hat{\mathbf{U}} \approx \hat{\mathbf{I}} + \frac{1}{2J_0} \left[\mathbf{H} \otimes \mathbf{a}_0^{(3)} + \mathbf{a}_0^{(3)} \otimes \mathbf{H} \right]$ as an *approximate* expression for the right stretch tensor of leading order in $\mathbf{H}/J_0$, because its square agrees with the exact expression for $\hat{\mathbf{C}}$ up to terms of order $\mathcal{O}(\mathbf{H}^2/J_0^2)$. Therefore, we obtain $\hat{\mathbf{E}}_B \approx \frac{1}{2J_0} \left[\mathbf{H} \otimes \mathbf{a}_0^{(3)} + \mathbf{a}_0^{(3)} \otimes \mathbf{H} \right]$ as an *approximate* expression for the Biot strain, which reduces to (19) for $J_0 \approx 1$ and provides an alternative interpretation of (19). The solution of the spectral problem for the approximate Biot strain tensor consistently yields the same eigenvalues and eigenvectors obtained from the formulas given above by inserting the small strain approximation $E_{33} \approx H_3/J_0$.

Similarily we may use $\hat{\mathbf{R}}_{pd}(\xi_1, \xi_2, s, t) \approx \hat{\mathbf{R}}_{rel}(s, t)$ to approximate the rotational part of the polar decomposition of $\hat{\mathbf{F}}$, which altogether yields the approximation $\hat{\mathbf{F}} \approx \hat{\mathbf{R}}_{rel} \cdot \left(\hat{\mathbf{I}} + \frac{1}{2J_0} \left[\mathbf{H} \otimes \mathbf{a}_0^{(3)} + \mathbf{a}_0^{(3)} \otimes \mathbf{H} \right] \right)$ of the deformation gradient. Insight into the precise nature of this approximation may be obtained by considering $\hat{\mathbf{R}}_{pd} = \hat{\mathbf{F}} \cdot \hat{\mathbf{U}}^{-1}$ with $\hat{\mathbf{F}}$ given exactly by (16) and $\hat{\mathbf{U}}$ approximated as mentioned above. Decomposing the tensor $\mathbf{H} \otimes \mathbf{a}_0^{(3)}$ into its symmetric and skew parts and neglecting terms of order $\mathcal{O}(\mathbf{H}^2/J_0^2)$ one may derive the approximate relation $\hat{\mathbf{R}}_{rel}^T \cdot \hat{\mathbf{R}}_{pd} \approx \hat{\mathbf{I}} + \frac{1}{2J_0} \left[\mathbf{H}_\perp \otimes \mathbf{a}_0^{(3)} - \mathbf{a}_0^{(3)} \otimes \mathbf{H}_\perp \right]$, from which we obtain the error estimate $\| \hat{\mathbf{R}}_{pd} - \hat{\mathbf{R}}_{rel} \| = \mathcal{O}(\| \mathbf{H}_\perp \|/J_0)$. This implies that the error of the approximation of $\hat{\mathbf{F}}$ suggested above is of the same order.

A.2 The material strain vector and the Biot strain

Following Kapania and Li (2003), Mata, Oller and Barbat (2007; 2008) use the spatial vector quantity

$$(\hat{\mathbf{F}} - \hat{\mathbf{R}}_{rel}) \cdot \mathbf{a}_0^{(3)} \;=\; \frac{1}{J_0} \hat{\mathbf{R}}_{rel} \cdot \mathbf{H} \;=\; \frac{1}{J_0} H_k \, \mathbf{a}^{(k)}$$

with $\hat{\mathbf{F}}$ given by a kinematically exact expression for the deformation gradient of a Cosserat rod equivalent to (16) to measure the strain at the individual points of a cross section. Its material counterpart $J_0^{-1} \hat{\mathbf{R}}_0^T \cdot \mathbf{H} = J_0^{-1} H_k \, \mathbf{e}_k$ as well as objective rates of both vector quantities are then used by these

authors to formulate inelastic constitutive laws for their rod model on the 3D level, which are required for a subsequent numerical evaluation of the spatial stress resultants and couples of the rod in its deformed configurations by numerical integration over the cross section areas.

Following our discussion of the Biot strain and its approximation given above, one recognizes that the strain measure used by Mata, Oller and Barbat (2008) likewise may be interpreted in terms of an approximation of the Biot strain via

$$\hat{\mathbf{F}} - \hat{\mathbf{R}}_{rel} \;\; \approx \;\; \hat{\mathbf{F}} - \hat{\mathbf{R}}_{pd} \;\; = \;\; \hat{\mathbf{R}}_{pd} \cdot \hat{\mathbf{E}}_B \;\; \approx \;\; \hat{\mathbf{R}}_{rel} \cdot \hat{\mathbf{E}}_B \; .$$

Using $\hat{\mathbf{F}} - \hat{\mathbf{R}}_{pd}$ as a strain measure is directly related to the geometric idea to quantify the strains caused by the deformation of a body by the deviation of a deformation mapping to a rigid body motion, as discussed by Chao et al. (2010). For a given deformation gradient $\hat{\mathbf{F}}$ with positive determinant, this deviation may be measured by the distance of $\hat{\mathbf{F}}$ to the group $\mathsf{SO}(3)$ of proper rotations defined as $\min_{\hat{\mathbf{R}} \in \mathsf{SO}(3)} \|\hat{\mathbf{F}} - \hat{\mathbf{R}}\|_F$, where $\| \cdot \|_F$ denotes the Frobenius norm. It can be shown that the minimum is actually reached for the unique rotation $\hat{\mathbf{R}} = \hat{\mathbf{R}}_{pd}$ provided implicitly by the polar decomposition of $\hat{\mathbf{F}}$, such that $\min_{\hat{\mathbf{R}} \in \mathsf{SO}(3)} \|\hat{\mathbf{F}} - \hat{\mathbf{R}}\|_F \;=\; \|\hat{\mathbf{R}}_{pd} \cdot (\hat{\mathbf{U}} - \hat{\mathbf{I}})\|_F \;=\; \|\hat{\mathbf{E}}_B\|_F$ holds due to the invariance of the norm under rotations. Altogether these considerations, combined with the approximation $\hat{\mathbf{R}}_{pd} \approx \hat{\mathbf{R}}_{rel}$, provide a geometric interpretation for the strain measure considered by Mata, Oller and Barbat (2008) and its relation to the Biot strain.

To compare the strain measure proposed by Mata, Oller and Barbat (2008) to our approximate strain measure given by (19) we consider $\hat{\mathbf{F}} = \hat{\mathbf{R}}_{pd} \cdot \hat{\mathbf{U}}$ constructed from $\hat{\mathbf{R}}_{pd} \approx \hat{\mathbf{R}}_{rel}$ and $\hat{\mathbf{U}} \approx \hat{\mathbf{I}} + \frac{1}{2J_0} \left[\mathbf{H} \otimes \mathbf{a}_0^{(3)} + \mathbf{a}_0^{(3)} \otimes \mathbf{H} \right]$ as suggested previously in accordance with the small strain approximation $\hat{\mathbf{E}}_B$. This leads to the (spatial) vectorial strain quantity[20]

$$(\hat{\mathbf{F}} - \hat{\mathbf{R}}_{rel}) \cdot \mathbf{a}_0^{(3)} \;\; = \;\; \frac{1}{J_0} \left(\frac{H_\alpha}{2} \, \mathbf{a}^{(\alpha)} + H_3 \, \mathbf{a}^{(3)} \right) \; ,$$

which differs from the definition chosen by Mata, Oller and Barbat (2008) by weighting the strain vector components H_α related to transverse shear and twisting by a factor $\frac{1}{2}$ relative to the component H_3 representing normal strains goverened by extension and bending.

---

[20]One obtains exactly the same result if one adds the modification $\hat{\mathbf{E}}' = \hat{\mathbf{E}} - \nu E_{33} \left[\hat{\mathbf{I}} - \mathbf{a}^{(3)} \otimes \mathbf{a}^{(3)} \right]$ according to (24) to the strain. This shows that measuring cross-sectional strains in terms of a vector quantity as suggested by Kapania and Li (2003) and Mata, Oller and Barbat (2008) is by construction *insensitive to lateral contraction effects*, which on the contrary are accounted for by our energy based approach.

A.3 The Biot stress and its approximation

In some works dealing with geometrically exact rods, e.g. in the articles of Irschik and Gerstmayr (2009) and Humer and Irschik (2011), 3D stress distributions within cross sections are analyzed in terms of the (unsymmetric) *Biot stress* tensor $\hat{\mathbf{T}}_B := \hat{\mathbf{R}}_{pd}^T \cdot \hat{\mathbf{P}} = \hat{\mathbf{U}} \cdot \hat{\mathbf{S}}$, which is related to the (*true*) Cauchy stress $\hat{\boldsymbol{\sigma}}$ via the co-rotational stress tensor $\hat{\mathbf{R}}_{pd}^T \cdot \hat{\boldsymbol{\sigma}} \cdot \hat{\mathbf{R}}_{pd} = J^{-1} \hat{\mathbf{T}}_B \cdot \hat{\mathbf{U}}$. The stress tensor $\hat{\mathbf{T}}_B$ as well as its *symmetric* part $\hat{\mathbf{T}}_B^{(s)} := \frac{1}{2}(\hat{\mathbf{T}}_B + \hat{\mathbf{T}}_B^T)$ are *both* work–conjugate stresses related to the Biot strain $\hat{\mathbf{E}}_B$, as both yield identical virtual work expressions due to the identity $\left[\hat{\mathbf{T}}_B - \hat{\mathbf{T}}_B^{(s)}\right] : \delta \hat{\mathbf{E}}_B = 0$.

Small strain approximations of these stress quantities are obtained by substituting $\hat{\mathbf{U}} \approx \hat{\mathbf{I}}$ (implying $\hat{\mathbf{F}} \approx \hat{\mathbf{R}}_{pd}$ and $J \approx 1$) into the various transformation identities for the stresses as given above. This yields the set of approximate relations $\hat{\mathbf{T}}_B \approx \hat{\mathbf{R}}_{pd}^T \cdot \hat{\boldsymbol{\sigma}} \cdot \hat{\mathbf{R}}_{pd} \approx \hat{\mathbf{T}}_B^{(s)} \approx \hat{\mathbf{S}}$, which are valid to leading order, analogous to the approximate relations $\hat{\mathbf{E}}_B \approx \hat{\mathbf{E}}$ for the corresponding strain quantities. The approximate stress relations (21) are obtained by the additional approximation $\hat{\mathbf{F}} \cdot \hat{\mathbf{U}}^{-1} = \hat{\mathbf{R}}_{pd} \approx \hat{\mathbf{R}}_{rel}$, likewise valid to the same order, which effectively amounts to applying the approximation $\hat{\mathbf{F}} \approx \hat{\mathbf{R}}_{rel}$ (implying $J \approx 1$) within all transformations of stress tensors.

In summary, due to the assumption of small strains, the Biot and 2nd Piola–Kichhoff stress tensors approximately coincide to leading order (i.e.: $\hat{\mathbf{T}}_B \approx \hat{\mathbf{S}}$). Moreover, both stresses correspond to the approximate co-rotational stress tensor $\hat{\mathbf{R}}_{rel}^T \cdot \hat{\boldsymbol{\sigma}} \cdot \hat{\mathbf{R}}_{rel}$ given by the components of the Cauchy stress w.r.t. the approximate material basis (i.e.: $\mathbf{G}_k \approx \mathbf{a}_0^{(k)} \approx \mathbf{G}^k$) provided by the reference frames $\hat{\mathbf{R}}_0(s) = \mathbf{a}_0^{(k)}(s) \otimes \mathbf{e}_k$ of the undeformed rod.

Published reports of the Fraunhofer ITWM

The PDF-files of the following reports are available under:

www.itwm.fraunhofer.de/presse-und-publikationen/

1. D. Hietel, K. Steiner, J. Struckmeier
A Finite - Volume Particle Method for Compressible Flows
(19 pages, 1998)

2. M. Feldmann, S. Seibold
Damage Diagnosis of Rotors: Application of Hilbert Transform and Multi-Hypothesis Testing
Keywords: Hilbert transform, damage diagnosis, Kalman filtering, non-linear dynamics
(23 pages, 1998)

3. Y. Ben-Haim, S. Seibold
Robust Reliability of Diagnostic Multi-Hypothesis Algorithms: Application to Rotating Machinery
Keywords: Robust reliability, convex models, Kalman filtering, multi-hypothesis diagnosis, rotating machinery, crack diagnosis
(24 pages, 1998)

4. F.-Th. Lentes, N. Siedow
Three-dimensional Radiative Heat Transfer in Glass Cooling Processes
(23 pages, 1998)

5. A. Klar, R. Wegener
A hierarchy of models for multilane vehicular traffic
Part I: Modeling
(23 pages, 1998)

Part II: Numerical and stochastic investigations
(17 pages, 1998)

6. A. Klar, N. Siedow
Boundary Layers and Domain Decomposition for Radiative Heat Transfer and Diffusion Equations: Applications to Glass Manufacturing Processes
(24 pages, 1998)

7. I. Choquet
Heterogeneous catalysis modelling and numerical simulation in rarified gas flows Part I: Coverage locally at equilibrium
(24 pages, 1998)

8. J. Ohser, B. Steinbach, C. Lang
Efficient Texture Analysis of Binary Images
(17 pages, 1998)

9. J. Orlik
Homogenization for viscoelasticity of the integral type with aging and shrinkage
(20 pages, 1998)

10. J. Mohring
Helmholtz Resonators with Large Aperture
(21 pages, 1998)

11. H. W. Hamacher, A. Schöbel
On Center Cycles in Grid Graphs
(15 pages, 1998)

12. H. W. Hamacher, K.-H. Küfer
Inverse radiation therapy planning - a multiple objective optimisation approach
(14 pages, 1999)

13. C. Lang, J. Ohser, R. Hilfer
On the Analysis of Spatial Binary Images
(20 pages, 1999)

14. M. Junk
On the Construction of Discrete Equilibrium Distributions for Kinetic Schemes
(24 pages, 1999)

15. M. Junk, S. V. Raghurame Rao
A new discrete velocity method for Navier-Stokes equations
(20 pages, 1999)

16. H. Neunzert
Mathematics as a Key to Key Technologies
(39 pages, 1999)

17. J. Ohser, K. Sandau
Considerations about the Estimation of the Size Distribution in Wicksell's Corpuscle Problem
(18 pages, 1999)

18. E. Carrizosa, H. W. Hamacher, R. Klein, S. Nickel
Solving nonconvex planar location problems by finite dominating sets
Keywords: Continuous Location, Polyhedral Gauges, Finite Dominating Sets, Approximation, Sandwich Algorithm, Greedy Algorithm
(19 pages, 2000)

19. A. Becker
A Review on Image Distortion Measures
Keywords: Distortion measure, human visual system
(26 pages, 2000)

20. H. W. Hamacher, M. Labbé, S. Nickel, T. Sonneborn
Polyhedral Properties of the Uncapacitated Multiple Allocation Hub Location Problem
Keywords: integer programming, hub location, facility location, valid inequalities, facets, branch and cut
(21 pages, 2000)

21. H. W. Hamacher, A. Schöbel
Design of Zone Tariff Systems in Public Transportation
(30 pages, 2001)

22. D. Hietel, M. Junk, R. Keck, D. Teleaga
The Finite-Volume-Particle Method for Conservation Laws
(16 pages, 2001)

23. T. Bender, H. Hennes, J. Kalcsics, M. T. Melo, S. Nickel
Location Software and Interface with GIS and Supply Chain Management
Keywords: facility location, software development, geographical information systems, supply chain management
(48 pages, 2001)

24. H. W. Hamacher, S. A. Tjandra
Mathematical Modelling of Evacuation Problems: A State of Art
(44 pages, 2001)

25. J. Kuhnert, S. Tiwari
Grid free method for solving the Poisson equation
Keywords: Poisson equation, Least squares method, Grid free method
(19 pages, 2001)

26. T. Götz, H. Rave, D. Reinel-Bitzer, K. Steiner, H. Tiemeier
Simulation of the fiber spinning process
Keywords: Melt spinning, fiber model, Lattice Boltzmann, CFD
(19 pages, 2001)

27. A. Zemitis
On interaction of a liquid film with an obstacle
Keywords: impinging jets, liquid film, models, numerical solution, shape
(22 pages, 2001)

28. I. Ginzburg, K. Steiner
Free surface lattice-Boltzmann method to model the filling of expanding cavities by Bingham Fluids
Keywords: Generalized LBE, free-surface phenomena, interface boundary conditions, filling processes, Bingham viscoplastic model, regularized models
(22 pages, 2001)

29. H. Neunzert
»Denn nichts ist für den Menschen als Menschen etwas wert, was er nicht mit Leidenschaft tun kann«
Vortrag anlässlich der Verleihung des Akademiepreises des Landes Rheinland-Pfalz am 21.11.2001
Keywords: Lehre, Forschung, angewandte Mathematik, Mehrskalenanalyse, Strömungsmechanik
(18 pages, 2001)

30. J. Kuhnert, S. Tiwari
Finite pointset method based on the projection method for simulations of the incompressible Navier-Stokes equations
Keywords: Incompressible Navier-Stokes equations, Meshfree method, Projection method, Particle scheme, Least squares approximation
AMS subject classification: 76D05, 76M28
(25 pages, 2001)

31. R. Korn, M. Krekel
Optimal Portfolios with Fixed Consumption or Income Streams
Keywords: Portfolio optimisation, stochastic control, HJB equation, discretisation of control problems
(23 pages, 2002)

32. M. Krekel
Optimal portfolios with a loan dependent credit spread
Keywords: Portfolio optimisation, stochastic control, HJB equation, credit spread, log utility, power utility, non-linear wealth dynamics
(25 pages, 2002)

33. J. Ohser, W. Nagel, K. Schladitz
The Euler number of discretized sets – on the choice of adjacency in homogeneous lattices
Keywords: image analysis, Euler number, neighborhod relationships, cuboidal lattice
(32 pages, 2002)

34. I. Ginzburg, K. Steiner

Lattice Boltzmann Model for Free-Surface flow and Its Application to Filling Process in Casting

Keywords: Lattice Boltzmann models; free-surface phenomena; interface boundary conditions; filling processes; injection molding; volume of fluid method; interface boundary conditions; advection-schemes; upwind-schemes
(54 pages, 2002)

35. M. Günther, A. Klar, T. Materne,
    R. Wegener

Multivalued fundamental diagrams and stop and go waves for continuum traffic equations

Keywords: traffic flow, macroscopic equations, kinetic derivation, multivalued fundamental diagram, stop and go waves, phase transitions
(25 pages, 2002)

36. S. Feldmann, P. Lang, D. Prätzel-Wolters

Parameter influence on the zeros of network determinants

Keywords: Networks, Equicofactor matrix polynomials, Realization theory, Matrix perturbation theory
(30 pages, 2002)

37. K. Koch, J. Ohser, K. Schladitz

Spectral theory for random closed sets and estimating the covariance via frequency space

Keywords: Random set, Bartlett spectrum, fast Fourier transform, power spectrum
(28 pages, 2002)

38. D. d'Humières, I. Ginzburg

Multi-reflection boundary conditions for lattice Boltzmann models

Keywords: lattice Boltzmann equation, boudary conditions, bounce-back rule, Navier-Stokes equation
(72 pages, 2002)

39. R. Korn

Elementare Finanzmathematik

Keywords: Finanzmathematik, Aktien, Optionen, Portfolio-Optimierung, Börse, Lehrerweiterbildung, Mathematikunterricht
(98 pages, 2002)

40. J. Kallrath, M. C. Müller, S. Nickel

**Batch Presorting Problems:
Models and Complexity Results**

Keywords: Complexity theory, Integer programming, Assigment, Logistics
(19 pages, 2002)

41. J. Linn

On the frame-invariant description of the phase space of the Folgar-Tucker equation

Key words: fiber orientation, Folgar-Tucker equation, injection molding
(5 pages, 2003)

42. T. Hanne, S. Nickel

A Multi-Objective Evolutionary Algorithm for Scheduling and Inspection Planning in Software Development Projects

Key words: multiple objective programming, project management and scheduling, software development, evolutionary algorithms, efficient set
(29 pages, 2003)

43. T. Bortfeld , K.-H. Küfer, M. Monz,
    A. Scherrer, C. Thieke, H. Trinkaus

Intensity-Modulated Radiotherapy - A Large Scale Multi-Criteria Programming Problem

Keywords: multiple criteria optimization, representative systems of Pareto solutions, adaptive triangulation, clustering and disaggregation techniques, visualization of Pareto solutions, medical physics, external beam radiotherapy planning, intensity modulated radiotherapy
(31 pages, 2003)

44. T. Halfmann, T. Wichmann

Overview of Symbolic Methods in Industrial Analog Circuit Design

Keywords: CAD, automated analog circuit design, symbolic analysis, computer algebra, behavioral modeling, system simulation, circuit sizing, macro modeling, differential-algebraic equations, index
(17 pages, 2003)

45. S. E. Mikhailov, J. Orlik

Asymptotic Homogenisation in Strength and Fatigue Durability Analysis of Composites

Keywords: multiscale structures, asymptotic homogenization, strength, fatigue, singularity, non-local conditions
(14 pages, 2003)

46. P. Domínguez-Marín, P. Hansen,
    N. Mladenovic , S. Nickel

Heuristic Procedures for Solving the Discrete Ordered Median Problem

Keywords: genetic algorithms, variable neighborhood search, discrete facility location
(31 pages, 2003)

47. N. Boland, P. Domínguez-Marín, S. Nickel,
    J. Puerto

Exact Procedures for Solving the Discrete Ordered Median Problem

Keywords: discrete location, Integer programming
(41 pages, 2003)

48. S. Feldmann, P. Lang

Padé-like reduction of stable discrete linear systems preserving their stability

Keywords: Discrete linear systems, model reduction, stability, Hankel matrix, Stein equation
(16 pages, 2003)

49. J. Kallrath, S. Nickel

A Polynomial Case of the Batch Presorting Problem

Keywords: batch presorting problem, online optimization, competetive analysis, polynomial algorithms, logistics
(17 pages, 2003)

50. T. Hanne, H. L. Trinkaus

**knowCube for MCDM –
Visual and Interactive Support for Multicriteria Decision Making**

Key words: Multicriteria decision making, knowledge management, decision support systems, visual interfaces, interactive navigation, real-life applications.
(26 pages, 2003)

51. O. Iliev, V. Laptev

On Numerical Simulation of Flow Through Oil Filters

Keywords: oil filters, coupled flow in plain and porous media, Navier-Stokes, Brinkman, numerical simulation
(8 pages, 2003)

52. W. Dörfler, O. Iliev, D. Stoyanov, D. Vassileva

On a Multigrid Adaptive Refinement Solver for Saturated Non-Newtonian Flow in Porous Media

Keywords: Nonlinear multigrid, adaptive refinement, non-Newtonian flow in porous media
(17 pages, 2003)

53. S. Kruse

On the Pricing of Forward Starting Options under Stochastic Volatility

Keywords: Option pricing, forward starting options, Heston model, stochastic volatility, cliquet options
(11 pages, 2003)

54. O. Iliev, D. Stoyanov

Multigrid – adaptive local refinement solver for incompressible flows

Keywords: Navier-Stokes equations, incompressible flow, projection-type splitting, SIMPLE, multigrid methods, adaptive local refinement, lid-driven flow in a cavity
(37 pages, 2003)

55. V. Starikovicius

The multiphase flow and heat transfer in porous media

Keywords: Two-phase flow in porous media, various formulations, global pressure, multiphase mixture model, numerical simulation
(30 pages, 2003)

56. P. Lang, A. Sarishvili, A. Wirsen

Blocked neural networks for knowledge extraction in the software development process

Keywords: Blocked Neural Networks, Nonlinear Regression, Knowledge Extraction, Code Inspection
(21 pages, 2003)

57. H. Knaf, P. Lang, S. Zeiser

Diagnosis aiding in Regulation Thermography using Fuzzy Logic

Keywords: fuzzy logic,knowledge representation, expert system
(22 pages, 2003)

58. M. T. Melo, S. Nickel, F. Saldanha da Gama

Largescale models for dynamic multicommodity capacitated facility location

Keywords: supply chain management, strategic planning, dynamic location, modeling
(40 pages, 2003)

59. J. Orlik

Homogenization for contact problems with periodically rough surfaces

Keywords: asymptotic homogenization, contact problems
(28 pages, 2004)

60. A. Scherrer, K.-H. Küfer, M. Monz,
    F. Alonso, T. Bortfeld

IMRT planning on adaptive volume structures – a significant advance of computational complexity

Keywords: Intensity-modulated radiation therapy (IMRT), inverse treatment planning, adaptive volume structures, hierarchical clustering, local refinement, adaptive clustering, convex programming, mesh generation, multi-grid methods
(24 pages, 2004)

61. D. Kehrwald

Parallel lattice Boltzmann simulation of complex flows

Keywords: Lattice Boltzmann methods, parallel computing, microstructure simulation, virtual material design, pseudo-plastic fluids, liquid composite moulding
(12 pages, 2004)

62. O. Iliev, J. Linn, M. Moog, D. Niedziela,
    V. Starikovicius

On the Performance of Certain Iterative Solvers for Coupled Systems Arising in Dis-

cretization of Non-Newtonian Flow Equations
Keywords: Performance of iterative solvers, Preconditioners, Non-Newtonian flow
(17 pages, 2004)

63. R. Ciegis, O. Iliev, S. Rief, K. Steiner
On Modelling and Simulation of Different Regimes for Liquid Polymer Moulding
Keywords: Liquid Polymer Moulding, Modelling, Simulation, Infiltration, Front Propagation, non-Newtonian flow in porous media
(43 pages, 2004)

64. T. Hanne, H. Neu
Simulating Human Resources in Software Development Processes
Keywords: Human resource modeling, software process, productivity, human factors, learning curve
(14 pages, 2004)

65. O. Iliev, A. Mikelic, P. Popov
Fluid structure interaction problems in deformable porous media: Toward permeability of deformable porous media
Keywords: fluid-structure interaction, deformable porous media, upscaling, linear elasticity, stokes, finite elements
(28 pages, 2004)

66. F. Gaspar, O. Iliev, F. Lisbona, A. Naumovich, P. Vabishchevich
On numerical solution of 1-D poroelasticity equations in a multilayered domain
Keywords: poroelasticity, multilayered material, finite volume discretization, MAC type grid
(41 pages, 2004)

67. J. Ohser, K. Schladitz, K. Koch, M. Nöthe
Diffraction by image processing and its application in materials science
Keywords: porous microstructure, image analysis, random set, fast Fourier transform, power spectrum, Bartlett spectrum
(13 pages, 2004)

68. H. Neunzert
Mathematics as a Technology: Challenges for the next 10 Years
Keywords: applied mathematics, technology, modelling, simulation, visualization, optimization, glass processing, spinning processes, fiber-fluid interaction, trubulence effects, topological optimization, multicriteria optimization, Uncertainty and Risk, financial mathematics, Malliavin calculus, Monte-Carlo methods, virtual material design, filtration, bio-informatics, system biology
(29 pages, 2004)

69. R. Ewing, O. Iliev, R. Lazarov, A. Naumovich
On convergence of certain finite difference discretizations for 1D poroelasticity interface problems
Keywords: poroelasticity, multilayered material, finite volume discretizations, MAC type grid, error estimates
(26 pages,2004)

70. W. Dörfler, O. Iliev, D. Stoyanov, D. Vassileva
On Efficient Simulation of Non-Newtonian Flow in Saturated Porous Media with a Multigrid Adaptive Refinement Solver
Keywords: Nonlinear multigrid, adaptive renement, non-Newtonian in porous media
(25 pages, 2004)

71. J. Kalcsics, S. Nickel, M. Schröder
Towards a Unified Territory Design Approach – Applications, Algorithms and GIS Integration
Keywords: territory desgin, political districting, sales territory alignment, optimization algorithms, Geographical Information Systems
(40 pages, 2005)

72. K. Schladitz, S. Peters, D. Reinel-Bitzer, A. Wiegmann, J. Ohser
Design of acoustic trim based on geometric modeling and flow simulation for non-woven
Keywords: random system of fibers, Poisson line process, flow resistivity, acoustic absorption, Lattice-Boltzmann method, non-woven
(21 pages, 2005)

73. V. Rutka, A. Wiegmann
Explicit Jump Immersed Interface Method for virtual material design of the effective elastic moduli of composite materials
Keywords: virtual material design, explicit jump immersed interface method, effective elastic moduli, composite materials
(22 pages, 2005)

74. T. Hanne
Eine Übersicht zum Scheduling von Baustellen
Keywords: Projektplanung, Scheduling, Bauplanung, Bauindustrie
(32 pages, 2005)

75. J. Linn
The Folgar-Tucker Model as a Differetial Algebraic System for Fiber Orientation Calculation
Keywords: fiber orientation, Folgar–Tucker model, invariants, algebraic constraints, phase space, trace stability
(15 pages, 2005)

76. M. Speckert, K. Dreßler, H. Mauch, A. Lion, G. J. Wierda
Simulation eines neuartigen Prüfsystems für Achserprobungen durch MKS-Modellierung einschließlich Regelung
Keywords: virtual test rig, suspension testing, multibody simulation, modeling hexapod test rig, optimization of test rig configuration
(20 pages, 2005)

77. K.-H. Küfer, M. Monz, A. Scherrer, P. Süss, F. Alonso, A.S.A. Sultan, Th. Bortfeld, D. Craft, Chr. Thieke
Multicriteria optimization in intensity modulated radiotherapy planning
Keywords: multicriteria optimization, extreme solutions, real-time decision making, adaptive approximation schemes, clustering methods, IMRT planning, reverse engineering
(51 pages, 2005)

78. S. Amstutz, H. Andrä
A new algorithm for topology optimization using a level-set method
Keywords: shape optimization, topology optimization, topological sensitivity, level-set
(22 pages, 2005)

79. N. Ettrich
Generation of surface elevation models for urban drainage simulation
Keywords: Flooding, simulation, urban elevation models, laser scanning
(22 pages, 2005)

80. H. Andrä, J. Linn, I. Matei, I. Shklyar, K. Steiner, E. Teichmann
OPTCAST – Entwicklung adäquater Strukturoptimierungsverfahren für Gießereien Technischer Bericht (KURZFASSUNG)
Keywords: Topologieoptimierung, Level-Set-Methode, Gießprozesssimulation, Gießtechnische Restriktionen, CAE-Kette zur Strukturoptimierung
(77 pages, 2005)

81. N. Marheineke, R. Wegener
Fiber Dynamics in Turbulent Flows Part I: General Modeling Framework
Keywords: fiber-fluid interaction; Cosserat rod; turbulence modeling; Kolmogorov's energy spectrum; double-velocity correlations; differentiable Gaussian fields
(20 pages, 2005)

Part II: Specific Taylor Drag
Keywords: flexible fibers; k-ε turbulence model; fiber-turbulence interaction scales; air drag; random Gaussian aerodynamic force; white noise; stochastic differential equations; ARMA process
(18 pages, 2005)

82. C. H. Lampert, O. Wirjadi
An Optimal Non-Orthogonal Separation of the Anisotropic Gaussian Convolution Filter
Keywords: Anisotropic Gaussian filter, linear filtering, orientation space, nD image processing, separable filters
(25 pages, 2005)

83. H. Andrä, D. Stoyanov
Error indicators in the parallel finite element solver for linear elasticity DDFEM
Keywords: linear elasticity, finite element method, hierarchical shape functions, domain decom-position, parallel implementation, a posteriori error estimates
(21 pages, 2006)

84. M. Schröder, I. Solchenbach
Optimization of Transfer Quality in Regional Public Transit
Keywords: public transit, transfer quality, quadratic assignment problem
(16 pages, 2006)

85. A. Naumovich, F. J. Gaspar
On a multigrid solver for the three-dimensional Biot poroelasticity system in multilayered domains
Keywords: poroelasticity, interface problem, multigrid, operator-dependent prolongation
(11 pages, 2006)

86. S. Panda, R. Wegener, N. Marheineke
Slender Body Theory for the Dynamics of Curved Viscous Fibers
Keywords: curved viscous fibers; fluid dynamics; Navier-Stokes equations; free boundary value problem; asymptotic expansions; slender body theory
(14 pages, 2006)

87. E. Ivanov, H. Andrä, A. Kudryavtsev
Domain Decomposition Approach for Automatic Parallel Generation of Tetrahedral Grids
Key words: Grid Generation, Unstructured Grid, Delaunay Triangulation, Parallel Programming, Domain Decomposition, Load Balancing
(18 pages, 2006)

88. S. Tiwari, S. Antonov, D. Hietel, J. Kuhnert, R. Wegener
A Meshfree Method for Simulations of Interactions between Fluids and Flexible Structures
Key words: Meshfree Method, FPM, Fluid Structure Interaction, Sheet of Paper, Dynamical Coupling
(16 pages, 2006)

89. R. Ciegis , O. Iliev, V. Starikovicius, K. Steiner
Numerical Algorithms for Solving Problems of Multiphase Flows in Porous Media

Keywords: nonlinear algorithms, finite-volume method, software tools, porous media, flows
(16 pages, 2006)

90. D. Niedziela, O. Iliev, A. Latz
On 3D Numerical Simulations of Viscoelastic Fluids
Keywords: non-Newtonian fluids, anisotropic viscosity, integral constitutive equation
(18 pages, 2006)

91. A. Winterfeld
Application of general semi-infinite Programming to Lapidary Cutting Problems
Keywords: large scale optimization, nonlinear programming, general semi-infinite optimization, design centering, clustering
(26 pages, 2006)

92. J. Orlik, A. Ostrovska
Space-Time Finite Element Approximation and Numerical Solution of Hereditary Linear Viscoelasticity Problems
Keywords: hereditary viscoelasticity; kern approximation by interpolation; space-time finite element approximation, stability and a priori estimate
(24 pages, 2006)

93. V. Rutka, A. Wiegmann, H. Andrä
EJIIM for Calculation of effective Elastic Moduli in 3D Linear Elasticity
Keywords: Elliptic PDE, linear elasticity, irregular domain, finite differences, fast solvers, effective elastic moduli
(24 pages, 2006)

94. A. Wiegmann, A. Zemitis
EJ-HEAT: A Fast Explicit Jump Harmonic Averaging Solver for the Effective Heat Conductivity of Composite Materials
Keywords: Stationary heat equation, effective thermal conductivity, explicit jump, discontinuous coefficients, virtual material design, microstructure simulation, EJ-HEAT
(21 pages, 2006)

95. A. Naumovich
On a finite volume discretization of the three-dimensional Biot poroelasticity system in multilayered domains
Keywords: Biot poroelasticity system, interface problems, finite volume discretization, finite difference method
(21 pages, 2006)

96. M. Krekel, J. Wenzel
A unified approach to Credit Default Swaption and Constant Maturity Credit Default Swap valuation
Keywords: LIBOR market model, credit risk, Credit Default Swaption, Constant Maturity Credit Default Swapmethod
(43 pages, 2006)

97. A. Dreyer
Interval Methods for Analog Circiuts
Keywords: interval arithmetic, analog circuits, tolerance analysis, parametric linear systems, frequency response, symbolic analysis, CAD, computer algebra
(36 pages, 2006)

98. N. Weigel, S. Weihe, G. Bitsch, K. Dreßler
Usage of Simulation for Design and Optimization of Testing
Keywords: Vehicle test rigs, MBS, control, hydraulics, testing philosophy
(14 pages, 2006)

99. H. Lang, G. Bitsch, K. Dreßler, M. Speckert
Comparison of the solutions of the elastic and elastoplastic boundary value problems
Keywords: Elastic BVP, elastoplastic BVP, variational inequalities, rate-independency, hysteresis, linear kinematic hardening, stop- and play-operator
(21 pages, 2006)

100. M. Speckert, K. Dreßler, H. Mauch
MBS Simulation of a hexapod based suspension test rig
Keywords: Test rig, MBS simulation, suspension, hydraulics, controlling, design optimization
(12 pages, 2006)

101. S. Azizi Sultan, K.-H. Küfer
A dynamic algorithm for beam orientations in multicriteria IMRT planning
Keywords: radiotherapy planning, beam orientation optimization, dynamic approach, evolutionary algorithm, global optimization
(14 pages, 2006)

102. T. Götz, A. Klar, N. Marheineke, R. Wegener
A Stochastic Model for the Fiber Lay-down Process in the Nonwoven Production
Keywords: fiber dynamics, stochastic Hamiltonian system, stochastic averaging
(17 pages, 2006)

103. Ph. Süss, K.-H. Küfer
Balancing control and simplicity: a variable aggregation method in intensity modulated radiation therapy planning
Keywords: IMRT planning, variable aggregation, clustering methods
(22 pages, 2006)

104. A. Beaudry, G. Laporte, T. Melo, S. Nickel
Dynamic transportation of patients in hospitals
Keywords: in-house hospital transportation, dial-a-ride, dynamic mode, tabu search
(37 pages, 2006)

105. Th. Hanne
Applying multiobjective evolutionary algorithms in industrial projects
Keywords: multiobjective evolutionary algorithms, discrete optimization, continuous optimization, electronic circuit design, semi-infinite programming, scheduling
(18 pages, 2006)

106. J. Franke, S. Halim
Wild bootstrap tests for comparing signals and images
Keywords: wild bootstrap test, texture classification, textile quality control, defect detection, kernel estimate, nonparametric regression
(13 pages, 2007)

107. Z. Drezner, S. Nickel
Solving the ordered one-median problem in the plane
Keywords: planar location, global optimization, ordered median, big triangle small triangle method, bounds, numerical experiments
(21 pages, 2007)

108. Th. Götz, A. Klar, A. Unterreiter, R. Wegener
Numerical evidence for the non-existing of solutions of the equations desribing rotational fiber spinning
Keywords: rotational fiber spinning, viscous fibers, boundary value problem, existence of solutions
(11 pages, 2007)

109. Ph. Süss, K.-H. Küfer
Smooth intensity maps and the Bortfeld-Boyer sequencer
Keywords: probabilistic analysis, intensity modulated radiotherapy treatment (IMRT), IMRT plan application, step-and-shoot sequencing
(8 pages, 2007)

110. E. Ivanov, O. Gluchshenko, H. Andrä, A. Kudryavtsev
Parallel software tool for decomposing and meshing of 3d structures
Keywords: a-priori domain decomposition, unstructured grid, Delaunay mesh generation
(14 pages, 2007)

111. O. Iliev, R. Lazarov, J. Willems
Numerical study of two-grid preconditioners for 1d elliptic problems with highly oscillating discontinuous coefficients
Keywords: two-grid algorithm, oscillating coefficients, preconditioner
(20 pages, 2007)

112. L. Bonilla, T. Götz, A. Klar, N. Marheineke, R. Wegener
Hydrodynamic limit of the Fokker-Planck-equation describing fiber lay-down processes
Keywords: stochastic dierential equations, Fokker-Planck equation, asymptotic expansion, Ornstein-Uhlenbeck process
(17 pages, 2007)

113. S. Rief
Modeling and simulation of the pressing section of a paper machine
Keywords: paper machine, computational fluid dynamics, porous media
(41 pages, 2007)

114. R. Ciegis, O. Iliev, Z. Lakdawala
On parallel numerical algorithms for simulating industrial filtration problems
Keywords: Navier-Stokes-Brinkmann equations, finite volume discretization method, SIMPLE, parallel computing, data decomposition method
(24 pages, 2007)

115. N. Marheineke, R. Wegener
Dynamics of curved viscous fibers with surface tension
Keywords: Slender body theory, curved viscous bers with surface tension, free boundary value problem
(25 pages, 2007)

116. S. Feth, J. Franke, M. Speckert
Resampling-Methoden zur mse-Korrektur und Anwendungen in der Betriebsfestigkeit
Keywords: Weibull, Bootstrap, Maximum-Likelihood, Betriebsfestigkeit
(16 pages, 2007)

117. H. Knaf
Kernel Fisher discriminant functions – a concise and rigorous introduction
Keywords: wild bootstrap test, texture classification, textile quality control, defect detection, kernel estimate, nonparametric regression
(30 pages, 2007)

118. O. Iliev, I. Rybak
On numerical upscaling for flows in heterogeneous porous media
Keywords: numerical upscaling, heterogeneous porous media, single phase flow, Darcy's law, multiscale problem, effective permeability, multipoint flux approximation, anisotropy
(17 pages, 2007)

119. O. Iliev, I. Rybak
On approximation property of multipoint flux approximation method
Keywords: Multipoint flux approximation, finite volume method, elliptic equation, discontinuous tensor coefficients, anisotropy
(15 pages, 2007)

120. O. Iliev, I. Rybak, J. Willems
On upscaling heat conductivity for a class of industrial problems
Keywords: Multiscale problems, effective heat conductivity, numerical upscaling, domain decomposition
(21 pages, 2007)

121. R. Ewing, O. Iliev, R. Lazarov, I. Rybak
On two-level preconditioners for flow in porous media
Keywords: Multiscale problem, Darcy's law, single phase flow, anisotropic heterogeneous porous media, numerical upscaling, multigrid, domain decomposition, efficient preconditioner
(18 pages, 2007)

122. M. Brickenstein, A. Dreyer
POLYBORI: A Gröbner basis framework for Boolean polynomials
Keywords: Gröbner basis, formal verification, Boolean polynomials, algebraic cryptoanalysis, satisfiability
(23 pages, 2007)

123. O. Wirjadi
Survey of 3d image segmentation methods
Keywords: image processing, 3d, image segmentation, binarization
(20 pages, 2007)

124. S. Zeytun, A. Gupta
A Comparative Study of the Vasicek and the CIR Model of the Short Rate
Keywords: interest rates, Vasicek model, CIR-model, calibration, parameter estimation
(17 pages, 2007)

125. G. Hanselmann, A. Sarishvili
Heterogeneous redundancy in software quality prediction using a hybrid Bayesian approach
Keywords: reliability prediction, fault prediction, non-homogeneous poisson process, Bayesian model averaging
(17 pages, 2007)

126. V. Maag, M. Berger, A. Winterfeld, K.-H. Küfer
A novel non-linear approach to minimal area rectangular packing
Keywords: rectangular packing, non-overlapping constraints, non-linear optimization, regularization, relaxation
(18 pages, 2007)

127. M. Monz, K.-H. Küfer, T. Bortfeld, C. Thieke
Pareto navigation – systematic multi-criteria-based IMRT treatment plan determination
Keywords: convex, interactive multi-objective optimization, intensity modulated radiotherapy planning
(15 pages, 2007)

128. M. Krause, A. Scherrer
On the role of modeling parameters in IMRT plan optimization
Keywords: intensity-modulated radiotherapy (IMRT), inverse IMRT planning, convex optimization, sensitivity analysis, elasticity, modeling parameters, equivalent uniform dose (EUD)
(18 pages, 2007)

129. A. Wiegmann
Computation of the permeability of porous materials from their microstructure by FFF-Stokes
Keywords: permeability, numerical homogenization, fast Stokes solver
(24 pages, 2007)

130. T. Melo, S. Nickel, F. Saldanha da Gama
Facility Location and Supply Chain Management – A comprehensive review
Keywords: facility location, supply chain management, network design
(54 pages, 2007)

131. T. Hanne, T. Melo, S. Nickel
Bringing robustness to patient flow management through optimized patient transports in hospitals
Keywords: Dial-a-Ride problem, online problem, case study, tabu search, hospital logistics
(23 pages, 2007)

132. R. Ewing, O. Iliev, R. Lazarov, I. Rybak, J. Willems
An efficient approach for upscaling properties of composite materials with high contrast of coefficients
Keywords: effective heat conductivity, permeability of fractured porous media, numerical upscaling, fibrous insulation materials, metal foams
(16 pages, 2008)

133. S. Gelareh, S. Nickel
New approaches to hub location problems in public transport planning
Keywords: integer programming, hub location, transportation, decomposition, heuristic
(25 pages, 2008)

134. G. Thömmes, J. Becker, M. Junk, A. K. Vaikuntam, D. Kehrwald, A. Klar, K. Steiner, A. Wiegmann
A Lattice Boltzmann Method for immiscible multiphase flow simulations using the Level Set Method
Keywords: Lattice Boltzmann method, Level Set method, free surface, multiphase flow
(28 pages, 2008)

135. J. Orlik
Homogenization in elasto-plasticity
Keywords: multiscale structures, asymptotic homogenization, nonlinear energy
(40 pages, 2008)

136. J. Almquist, H. Schmidt, P. Lang, J. Deitmer, M. Jirstrand, D. Prätzel-Wolters, H. Becker
Determination of interaction between MCT1 and CAII via a mathematical and physiological approach
Keywords: mathematical modeling; model reduction; electrophysiology; pH-sensitive microelectrodes; proton antenna
(20 pages, 2008)

137. E. Savenkov, H. Andrä, O. Iliev
An analysis of one regularization approach for solution of pure Neumann problem
Keywords: pure Neumann problem, elasticity, regularization, finite element method, condition number
(27 pages, 2008)

138. O. Berman, J. Kalcsics, D. Krass, S. Nickel
The ordered gradual covering location problem on a network
Keywords: gradual covering, ordered median function, network location
(32 pages, 2008)

139. S. Gelareh, S. Nickel
Multi-period public transport design: A novel model and solution approaches
Keywords: Integer programming, hub location, public transport, multi-period planning, heuristics
(31 pages, 2008)

140. T. Melo, S. Nickel, F. Saldanha-da-Gama
Network design decisions in supply chain planning
Keywords: supply chain design, integer programming models, location models, heuristics
(20 pages, 2008)

141. C. Lautensack, A. Särkkä, J. Freitag, K. Schladitz
Anisotropy analysis of pressed point processes
Keywords: estimation of compression, isotropy test, nearest neighbour distance, orientation analysis, polar ice, Ripley's K function
(35 pages, 2008)

142. O. Iliev, R. Lazarov, J. Willems
A Graph-Laplacian approach for calculating the effective thermal conductivity of complicated fiber geometries
Keywords: graph laplacian, effective heat conductivity, numerical upscaling, fibrous materials
(14 pages, 2008)

143. J. Linn, T. Stephan, J. Carlsson, R. Bohlin
Fast simulation of quasistatic rod deformations for VR applications
Keywords: quasistatic deformations, geometrically exact rod models, variational formulation, energy minimization, finite differences, nonlinear conjugate gradients
(7 pages, 2008)

144. J. Linn, T. Stephan
Simulation of quasistatic deformations using discrete rod models
Keywords: quasistatic deformations, geometrically exact rod models, variational formulation, energy minimization, finite differences, nonlinear conjugate gradients
(9 pages, 2008)

145. J. Marburger, N. Marheineke, R. Pinnau
Adjoint based optimal control using mesh-less discretizations
Keywords: Mesh-less methods, particle methods, Eulerian-Lagrangian formulation, optimization strategies, adjoint method, hyperbolic equations
(14 pages, 2008)

146. S. Desmettre, J. Gould, A. Szimayer

Own-company stockholding and work effort preferences of an unconstrained executive

Keywords: optimal portfolio choice, executive compensation

(33 pages, 2008)

147. M. Berger, M. Schröder, K.-H. Küfer

A constraint programming approach for the two-dimensional rectangular packing problem with orthogonal orientations

Keywords: rectangular packing, orthogonal orientations non-overlapping constraints, constraint propagation

(13 pages, 2008)

148. K. Schladitz, C. Redenbach, T. Sych, M. Godehardt

Microstructural characterisation of open foams using 3d images

Keywords: virtual material design, image analysis, open foams

(30 pages, 2008)

149. E. Fernández, J. Kalcsics, S. Nickel, R. Ríos-Mercado

A novel territory design model arising in the implementation of the WEEE-Directive

Keywords: heuristics, optimization, logistics, recycling

(28 pages, 2008)

150. H. Lang, J. Linn

Lagrangian field theory in space-time for geometrically exact Cosserat rods

Keywords: Cosserat rods, geometrically exact rods, small strain, large deformation, deformable bodies, Lagrangian field theory, variational calculus

(19 pages, 2009)

151. K. Dreßler, M. Speckert, R. Müller, Ch. Weber

Customer loads correlation in truck engineering

Keywords: Customer distribution, safety critical components, quantile estimation, Monte-Carlo methods

(11 pages, 2009)

152. H. Lang, K. Dreßler

An improved multiaxial stress-strain correction model for elastic FE postprocessing

Keywords: Jiang's model of elastoplasticity, stress-strain correction, parameter identification, automatic differentiation, least-squares optimization, Coleman-Li algorithm

(6 pages, 2009)

153. J. Kalcsics, S. Nickel, M. Schröder

A generic geometric approach to territory design and districting

Keywords: Territory design, districting, combinatorial optimization, heuristics, computational geometry

(32 pages, 2009)

154. Th. Fütterer, A. Klar, R. Wegener

An energy conserving numerical scheme for the dynamics of hyperelastic rods

Keywords: Cosserat rod, hyperealstic, energy conservation, finite differences

(16 pages, 2009)

155. A. Wiegmann, L. Cheng, E. Glatt, O. Iliev, S. Rief

Design of pleated filters by computer simulations

Keywords: Solid-gas separation, solid-liquid separation, pleated filter, design, simulation

(21 pages, 2009)

156. A. Klar, N. Marheineke, R. Wegener

Hierarchy of mathematical models for production processes of technical textiles

Keywords: Fiber-fluid interaction, slender-body theory, turbulence modeling, model reduction, stochastic differential equations, Fokker-Planck equation, asymptotic expansions, parameter identification

(21 pages, 2009)

157. E. Glatt, S. Rief, A. Wiegmann, M. Knefel, E. Wegenke

Structure and pressure drop of real and virtual metal wire meshes

Keywords: metal wire mesh, structure simulation, model calibration, CFD simulation, pressure loss

(7 pages, 2009)

158. S. Kruse, M. Müller

Pricing American call options under the assumption of stochastic dividends – An application of the Korn-Rogers model

Keywords: option pricing, American options, dividends, dividend discount model, Black-Scholes model

(22 pages, 2009)

159. H. Lang, J. Linn, M. Arnold

Multibody dynamics simulation of geometrically exact Cosserat rods

Keywords: flexible multibody dynamics, large deformations, finite rotations, constrained mechanical systems, structural dynamics

(20 pages, 2009)

160. P. Jung, S. Leyendecker, J. Linn, M. Ortiz

Discrete Lagrangian mechanics and geometrically exact Cosserat rods

Keywords: special Cosserat rods, Lagrangian mechanics, Noether's theorem, discrete mechanics, frame-indifference, holonomic constraints

(14 pages, 2009)

161. M. Burger, K. Dreßler, A. Marquardt, M. Speckert

Calculating invariant loads for system simulation in vehicle engineering

Keywords: iterative learning control, optimal control theory, differential algebraic equations (DAEs)

(18 pages, 2009)

162. M. Speckert, N. Ruf, K. Dreßler

Undesired drift of multibody models excited by measured accelerations or forces

Keywords: multibody simulation, full vehicle model, force-based simulation, drift due to noise

(19 pages, 2009)

163. A. Streit, K. Dreßler, M. Speckert, J. Lichter, T. Zenner, P. Bach

Anwendung statistischer Methoden zur Erstellung von Nutzungsprofilen für die Auslegung von Mobilbaggern

Keywords: Nutzungsvielfalt, Kundenbeanspruchung, Bemessungsgrundlagen

(13 pages, 2009)

164. I. Correia, S. Nickel, F. Saldanha-da-Gama

The capacitated single-allocation hub location problem revisited: A note on a classical formulation

Keywords: Capacitated Hub Location, MIP formulations

(10 pages, 2009)

165. F. Yaneva, T. Grebe, A. Scherrer

An alternative view on global radiotherapy optimization problems

Keywords: radiotherapy planning, path-connected sublevelsets, modified gradient projection method, improving and feasible directions

(14 pages, 2009)

166. J. I. Serna, M. Monz, K.-H. Küfer, C. Thieke

Trade-off bounds and their effect in multi-criteria IMRT planning

Keywords: trade-off bounds, multi-criteria optimization, IMRT, Pareto surface

(15 pages, 2009)

167. W. Arne, N. Marheineke, A. Meister, R. Wegener

Numerical analysis of Cosserat rod and string models for viscous jets in rotational spinning processes

Keywords: Rotational spinning process, curved viscous fibers, asymptotic Cosserat models, boundary value problem, existence of numerical solutions

(18 pages, 2009)

168. T. Melo, S. Nickel, F. Saldanha-da-Gama

An LP-rounding heuristic to solve a multi-period facility relocation problem

Keywords: supply chain design, heuristic, linear programming, rounding

(37 pages, 2009)

169. I. Correia, S. Nickel, F. Saldanha-da-Gama

Single-allocation hub location problems with capacity choices

Keywords: hub location, capacity decisions, MILP formulations

(27 pages, 2009)

170. S. Acar, K. Natcheva-Acar

A guide on the implementation of the Heath-Jarrow-Morton Two-Factor Gaussian Short Rate Model (HJM-G2++)

Keywords: short rate model, two factor Gaussian, G2++, option pricing, calibration

(30 pages, 2009)

171. A. Szimayer, G. Dimitroff, S. Lorenz

A parsimonious multi-asset Heston model: calibration and derivative pricing

Keywords: Heston model, multi-asset, option pricing, calibration, correlation

(28 pages, 2009)

172. N. Marheineke, R. Wegener

Modeling and validation of a stochastic drag for fibers in turbulent flows

Keywords: fiber-fluid interactions, long slender fibers, turbulence modelling, aerodynamic drag, dimensional analysis, data interpolation, stochastic partial differential algebraic equation, numerical simulations, experimental validations

(19 pages, 2009)

173. S. Nickel, M. Schröder, J. Steeg

Planning for home health care services

Keywords: home health care, route planning, metaheuristics, constraint programming

(23 pages, 2009)

174. G. Dimitroff, A. Szimayer, A. Wagner

Quanto option pricing in the parsimonious Heston model

Keywords: Heston model, multi asset, quanto options, option pricing

(14 pages, 2009) 174. G. Dimitroff, A. Szimayer, A. Wagner

175. S. Herkt, K. Dreßler, R. Pinnau
Model reduction of nonlinear problems in structural mechanics
Keywords: flexible bodies, FEM, nonlinear model reduction, POD
(13 pages, 2009)

176. M. K. Ahmad, S. Didas, J. Iqbal
Using the Sharp Operator for edge detection and nonlinear diffusion
Keywords: maximal function, sharp function,image processing, edge detection, nonlinear diffusion
(17 pages, 2009)

177. M. Speckert, N. Ruf, K. Dreßler, R. Müller, C. Weber, S. Weihe
Ein neuer Ansatz zur Ermittlung von Erprobungslasten für sicherheitsrelevante Bauteile
Keywords: sicherheitsrelevante Bauteile, Kundenbeanspruchung, Festigkeitsverteilung, Ausfallwahrscheinlichkeit, Konfidenz, statistische Unsicherheit, Sicherheitsfaktoren
(16 pages, 2009)

178. J. Jegorovs
Wave based method: new applicability areas
Keywords: Elliptic boundary value problems, inhomogeneous Helmholtz type differential equations in bounded domains, numerical methods, wave based method, uniform B-splines
(10 pages, 2009)

179. H. Lang, M. Arnold
Numerical aspects in the dynamic simulation of geometrically exact rods
Keywords: Kirchhoff and Cosserat rods, geometrically exact rods, deformable bodies, multibody dynamics,artial differential algebraic equations, method of lines, time integration
(21 pages, 2009)

180. H. Lang
Comparison of quaternionic and rotation-free null space formalisms for multibody dynamics
Keywords: Parametrisation of rotations, differential-algebraic equations, multibody dynamics, constrained mechanical systems, Lagrangian mechanics
(40 pages, 2010)

181. S. Nickel, F. Saldanha-da-Gama, H.-P. Ziegler
Stochastic programming approaches for risk aware supply chain network design problems
Keywords: Supply Chain Management, multi-stage stochastic programming, financial decisions, risk
(37 pages, 2010)

182. P. Ruckdeschel, N. Horbenko
Robustness properties of estimators in generalized Pareto Models
Keywords: global robustness, local robustness, finite sample breakdown point, generalized Pareto distribution
(58 pages, 2010)

183. P. Jung, S. Leyendecker, J. Linn, M. Ortiz
A discrete mechanics approach to Cosserat rod theory – Part 1: static equilibria
Keywords: Special Cosserat rods; Lagrangian mechanics; Noether's theorem; discrete mechanics; frame-indifference; holonomic constraints; variational formulation
(35 pages, 2010)

184. R. Eymard, G. Printsypar
A proof of convergence of a finite volume scheme for modified steady Richards' equation describing transport processes in the pressing section of a paper machine
Keywords: flow in porous media, steady Richards' equation, finite volume methods, convergence of approximate solution
(14 pages, 2010)

185. P. Ruckdeschel
Optimally Robust Kalman Filtering
Keywords: robustness, Kalman Filter, innovation outlier, additive outlier
(42 pages, 2010)

186. S. Repke, N. Marheineke, R. Pinnau
On adjoint-based optimization of a free surface Stokes flow
Keywords: film casting process, thin films, free surface Stokes flow, optimal control, Lagrange formalism
(13 pages, 2010)

187. O. Iliev, R. Lazarov, J. Willems
Variational multiscale Finite Element Method for flows in highly porous media
Keywords: numerical upscaling, flow in heterogeneous porous media, Brinkman equations, Darcy's law, subgrid approximation, discontinuous Galerkin mixed FEM
(21 pages, 2010)

188. S. Desmettre, A. Szimayer
Work effort, consumption, and portfolio selection: When the occupational choice matters
Keywords: portfolio choice, work effort, consumption, occupational choice
(34 pages, 2010)

189. O. Iliev, Z. Lakdawala, V. Starikovicius
On a numerical subgrid upscaling algorithm for Stokes-Brinkman equations
Keywords: Stokes-Brinkman equations, subgrid approach, multiscale problems, numerical upscaling
(27 pages, 2010)

190. A. Latz, J. Zausch, O. Iliev
Modeling of species and charge transport in Li-Ion Batteries based on non-equilibrium thermodynamics
Keywords: lithium-ion battery, battery modeling, electrochemical simulation, concentrated electrolyte, ion transport
(8 pages, 2010)

191. P. Popov, Y. Vutov, S. Margenov, O. Iliev
Finite volume discretization of equations describing nonlinear diffusion in Li-Ion batteries
Keywords: nonlinear diffusion, finite volume discretization, Newton method, Li-Ion batteries
(9 pages, 2010)

192. W. Arne, N. Marheineke, R. Wegener
Asymptotic transition from Cosserat rod to string models for curved viscous inertial jets
Keywords: rotational spinning processes; inertial and viscous-inertial fiber regimes; asymptotic limits; slender-body theory; boundary value problems
(23 pages, 2010)

193. L. Engelhardt, M. Burger, G. Bitsch
Real-time simulation of multibody-systems for on-board applications
Keywords: multibody system simulation, real-time simulation, on-board simulation, Rosenbrock methods
(10 pages, 2010)

194. M. Burger, M. Speckert, K. Dreßler
Optimal control methods for the calculation of invariant excitation signals for multibody systems
Keywords: optimal control, optimization, mbs simulation, invariant excitation
(9 pages, 2010)

195. A. Latz, J. Zausch
Thermodynamic consistent transport theory of Li-Ion batteries
Keywords: Li-Ion batteries, nonequilibrium thermodynamics, thermal transport, modeling
(18 pages, 2010)

196. S. Desmettre
Optimal investment for executive stockholders with exponential utility
Keywords: portfolio choice, executive stockholder, work effort, exponential utility
(24 pages, 2010)

197. W. Arne, N. Marheineke, J. Schnebele, R. Wegener
Fluid-fiber-interactions in rotational spinning process of glass wool production
Keywords: Rotational spinning process, viscous thermal jets, fluid-fiber-interactions, two-way coupling, slender-body theory, Cosserat rods, drag models, boundary value problem, continuation method
(20 pages, 2010)

198. A. Klar, J. Maringer, R. Wegener
A 3d model for fiber lay-down in nonwoven production processes
Keywords: fiber dynamics, Fokker-Planck equations, diffusion limits
(15 pages, 2010)

199. Ch. Erlwein, M. Müller
A regime-switching regression model for hedge funds
Keywords: switching regression model, Hedge funds, optimal parameter estimation, filtering
(26 pages, 2011)

200. M. Dalheimer
Power to the people – Das Stromnetz der Zukunft
Keywords: Smart Grid, Stromnetz, Erneuerbare Energien, Demand-Side Management
(27 pages, 2011)

201. D. Stahl, J. Hauth
PF-MPC: Particle Filter-Model Predictive Control
Keywords: Model Predictive Control, Particle Filter, CSTR, Inverted Pendulum, Nonlinear Systems, Sequential Monte Carlo
(40 pages, 2011)

202. G. Dimitroff, J. de Kock
Calibrating and completing the volatility cube in the SABR Model
Keywords: stochastic volatility, SABR, volatility cube, swaption
(12 pages, 2011)

203. J.-P. Kreiss, T. Zangmeister
Quantification of the effectiveness of a safety function in passenger vehicles on the basis of real-world accident data
Keywords: logistic regression, safety function, real-world accident data, statistical modeling
(23 pages, 2011)

204. P. Ruckdeschel, T. Sayer, A. Szimayer

Pricing American options in the Heston model: a close look on incorporating correlation

Keywords: Heston model, American options, moment matching, correlation, tree method

(30 pages, 2011)

205. H. Ackermann, H. Ewe, K.-H. Küfer, M. Schröder

Modeling profit sharing in combinatorial exchanges by network flows

Keywords: Algorithmic game theory, profit sharing, combinatorial exchange, network flows, budget balance, core

(17 pages, 2011)

206. O. Iliev, G. Printsypar, S. Rief

A one-dimensional model of the pressing section of a paper machine including dynamic capillary effects

Keywords: steady modified Richards' equation, finite volume method, dynamic capillary pressure, pressing section of a paper machine

(29 pages, 2011)

207. I. Vecchio, K. Schladitz, M. Godehardt, M. J. Heneka

Geometric characterization of particles in 3d with an application to technical cleanliness

Keywords: intrinsic volumes, isoperimetric shape factors, bounding box, elongation, geodesic distance, technical cleanliness

(21 pages, 2011)

208. M. Burger, K. Dreßler, M. Speckert

Invariant input loads for full vehicle multibody system simulation

Keywords: multibody systems, full-vehicle simulation, optimal control

(8 pages, 2011)

209. H. Lang, J. Linn, M. Arnold

Multibody dynamics simulation of geometrically exact Cosserat rods

Keywords: flexible multibody dynamics, large deformations, finite rotations, constrained mechanical systems, structural dynamics

(28 pages, 2011)

210. G. Printsypar, R. Ciegis

On convergence of a discrete problem describing transport processes in the pressing section of a paper machine including dynamic capillary effects: one-dimensional case

Keywords: saturated and unsaturated fluid flow in porous media, Richards' approach, dynamic capillary pressure, finite volume methods, convergence of approximate solution

(24 pages, 2011)

211. O. Iliev, G. Printsypar, S. Rief

A two-cimensional model of the pressing section of a paper machine including dynamic capillary effects

Keywords: two-phase flow in porous media, steady modified Richards' equation, finite volume method, dynamic capillary pressure, pressing section of a paper machine, multipoint flux approximation

(44 pages, 2012)

212. M. Buck, O. Iliev, H. Andrä

Multiscale finite element coarse spaces for the analysis of linear elastic composites

Keywords: linear elasticity, domain decomposition, multiscale finite elements, robust coarse spaces, rigid body modes, discontinuous coefficients

(31 pages, 2012)

213. A. Wagner

Residual demand modeling and application to electricity pricing

Keywords: residual demand modeling, renewable infeed, wind infeed, solar infeed, electricity demand, German power market, merit-order effect

(28 pages, 2012)

214. O. Iliev, A. Latz, J. Zausch, S. Zhang

An overview on the usage of some model reduction approaches for simulations of Li-ion transport in batteries

Keywords: Li-ion batteries, porous electrode model, model reduction

(21 pages, 2012)

215. C. Zémerli, A. Latz, H. Andrä

Constitutive models for static granular systems and focus to the Jiang-Liu hyperelastic law

Keywords: granular elasticity, constitutive modelling, non-linear finite element method

(33 pages, 2012)

216. T. Gornak, J. L. Guermond, O. Iliev, P. D. Minev

A direction splitting approach for incompressible Brinkmann flow

Keywords: unsteady Navier-Stokes-Brinkman equations, direction splitting algorithms, nuclear reactors safety simulations

(16 pages, 2012)

217. Y. Efendiev, O. Iliev, C. Kronsbein

Multilevel Monte Carlo methods using ensemble level mixed MsFEM for two-phase flow and transport simulations

Keywords: two phase flow in porous media, uncertainty quantification, multilevel Monte Carlo

(28 pages, 2012)

218. J. Linn, H. Lang, A. Tuganov

Geometrically exact Cosserat rods with Kelvin-Voigt type viscous damping

Keywords: geometrically exact rods, viscous damping, Kelvin-Voigt model, material damping parameters

(10 pages, 2012)

219. M. Schulze, S. Dietz, J. Linn, H. Lang, A. Tuganov

Integration of nonlinear models of flexible body deformation in Multibody System Dynamics

Keywords: multibody system dynamics, flexible structures, discrete Cosserat rods, wind turbine rotor blades

(10 pages, 2012)

220. C. Weischedel, A. Tuganov, T. Hermansson, J. Linn, M. Wardetzky

Construction of discrete shell models by geometric finite differences

Keywords: geometrically exact shells, discrete differential geometry, rotation-free Kirchhoff model, triangular meshes

(10 pages, 2012)

221. M. Taralov, V. Taralova, P. Popov, O. Iliev, A. Latz, J. Zausch

Report on Finite Element Simulations of Electrochemical Processes in Li-ion Batteries with Thermic Effects

Keywords: Li-ion battery, FEM for nonlinear problems, FEM for discontinuous solutions, Nonlinear diffusion, Nonlinear interface conditions

(40 pages, 2012)

222. A. Scherrer, T. Grebe, F. Yaneva, K.-H. Küfer

Interactive DVH-based planning of intensity-modulated radiation therapy (IMRT)

Keywords: intensity-modulated radiation therapy (IMRT), cumulative dose-volume histogram (DVH), interactive IMRT planning, DVH-based planning criteria

(22 pages, 2012)

223. S. Frei, H. Andrä, R. Pinnau, O. Tse

An adjoint-based gradient-type algorithm for optimal fiber orientation in fiber-reinforced materials

Keywords: pde constrained optimization, fiber-reinforced materials, fiber orientation, linear elasticity, upscaling, adjoint-based optimization, microstructural optimization

(17 pages, 2012)

224. M. Kabel, H. Andrä

Fast numerical computation of precise bounds of effective elastic moduli

Keywords: composite materials, numerical homogenization, effective elasticity coefficients, Hashin-Shtrikman bounds, Lippmann-Schwinger equation, FFT

(16 pages, 2013)

225. J. Linn, H. Lang, A. Tuganov

Derivation of a viscoelastic constitutive model of Kelvin-Voigt type for Cosserat rods

Keywords: geometrically exact rods, viscoelasticity, Kelvin-Voigt model, nonlinear structural dynamics

(42 pages, 2013)

Status quo: February 2013